

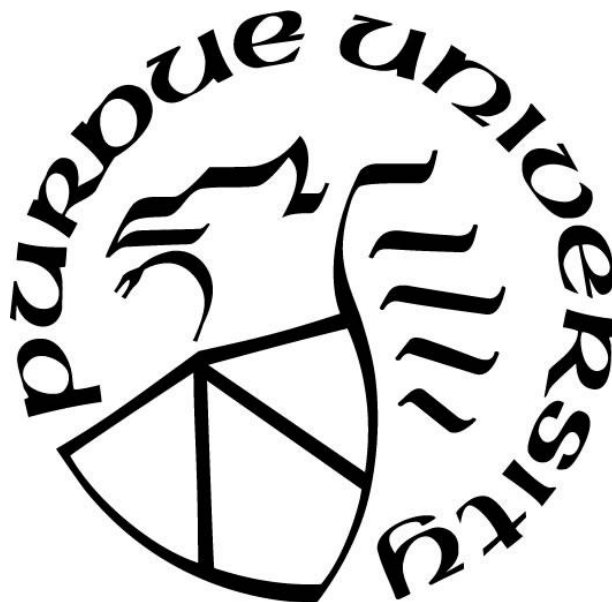
CHEMICAL HYDRIDE REACTOR DESIGNS FOR PORTABLE FUEL CELL DEVICES

by
Benjamin J. Hynes

A Thesis

*Submitted to the Faculty of Purdue University
In Partial Fulfillment of the Requirements for the degree of*

Master of Science in Aeronautics and Astronautics



School of Aeronautics and Astronautics

West Lafayette, Indiana

December 2019

THE PURDUE UNIVERSITY GRADUATE SCHOOL
STATEMENT OF COMMITTEE APPROVAL

Dr. Timothée Pourpoint, Chair

School of Aeronautics and Astronautics

Dr. Eric Dietz

Computer and Information Technology

Dr. Robert Orth

School of Aeronautics and Astronautics

Approved by:

Dr. Gregory Blaisdell

I dedicate this research to Jesus Christ.

ACKNOWLEDGMENTS

I would like to thank Dr. Pourpoint for guiding my research and providing support throughout my time at Purdue. I would also like to thank Dr. Orth and Dr. Dietz for serving on my committee and providing helpful contributions to my research. The work on this project would have been impossible without the support of Taylor Groom. I am grateful for all the time and support he put in to catch me up to speed and answer my unending questions. I would like to acknowledge Jason Gabl and Ben Whitehead for giving guidance in my experimentation and writing. I am also grateful for all of the other students in Pourpoint's group for answering questions and helping me come up with ideas. Finally I would like to thank the Purdue Military Research Initiative for funding my program and the U.S. Navy for giving me the time to pursue this degree.

TABLE OF CONTENTS

TABLE OF CONTENTS.....	5
LIST OF TABLES.....	7
LIST OF FIGURES	8
ABSTRACT.....	10
1. INTRODUCTION	11
2. BACKGROUND	14
2.1 Energy Storage in the Field.....	14
2.2 Fuel Cells	15
2.2.1 Proton Exchange Membrane Fuel Cell.....	16
2.3 Chemical Hydrides and Organic Acids.....	17
2.4 Design Targets	20
2.4.1 DoD Standards	23
3. REACTOR DESIGNS.....	25
3.1 Preliminary Designs.....	25
3.1.1 Liquid Mixing.....	27
3.1.2 Solid AB	28
3.1.3 Design Down Selection	30
3.2 Energy Density Assessment.....	30
3.2.1 Overall Energy Density Goal.....	30
3.2.2 Energy Density Comparison.....	31
3.3 Conceptual Design Trade Study	33
3.3.1 Model Selection	36
4. METHODOLOGY	37
4.1 Ammonia Borane Synthesis.....	37
4.2 Reactor Experimentation Setup	39
4.2.1 Test Stand	39
4.2.2 System Design and Procedures.....	40
4.3 Modeling Performance.....	43
5. RESULTS AND DISCUSSION.....	46

5.1	Liquid Mixing Designs	46
5.1.1	Single Fill.....	46
	Sensitivity Analysis.....	50
5.1.2	Regulated Fill.....	55
5.2	Solid AB.....	60
5.2.1	Applications.....	65
5.3	Revisit Trade Study.....	66
6.	CONCLUSIONS	69
6.1	Future Work.....	71
APPENDIX. MATLAB MODELS		73
REFERENCES		79

LIST OF TABLES

Table 1. Comparison of the different portable fuel cells.	15
Table 2. Go-no-go metrics for system.	22
Table 3. BB-2590 Performance Evaluation [36].	23
Table 4. Energy density prediction.	32
Table 5. Design parameter weighting.	34
Table 6. Preliminary Pugh Chart analysis.....	35
Table 7. Reactor Sizing process.....	48
Table 8. Prototype design values.	51
Table 9. 20 gram AB reactor design.	58
Table 10. Concluding Pugh chart analysis.....	67

LIST OF FIGURES

Figure 1.1. Gravimetric and volumetric energy densities for hydrogen storage materials, modified [28].	18
Figure 2.2. AB solution delivered by spring loaded piston.	20
Figure 2.3. AB solution delivered by peristaltic pump.	21
Figure 2.4. SPM-622 harvesting power to charge military equipment. [34]	22
Figure 3.1. Design breakdown based on hydrolysis control method.	26
Figure 3.2. A) Externally driven AB solution to reactor; B) Pressurized delivery of AB solution from reactor hydrogen.	28
Figure 3.3. E) Controlled release of AB in solution; F) Controlled exposure of AB to solution.	29
Figure 3.4. G) Pressure dependent exposure of AB to acidic solution.	30
Figure 3.5. Hydrogen density assessment.	33
Figure 4.1. Ammonia Borane Filtration.	37
Figure 4.2. THF evaporation.	38
Figure 4.3. Test stand plumbing and instrumentation diagram.	39
Figure 4.4. Plumbing and instrumentation diagram for A design.	40
Figure 4.5. Plumbing and instrumentation diagram for B design.	41
Figure 4.6. Pressed AB pellet.	42
Figure 4.7. Plumbing and instrumentation diagram for AB pellet design.	43
Figure 4.8. Single pressurization: MATLAB flow diagram.	44
Figure 4.9. Regulated pressurization: MATLAB flow diagram.	45
Figure 5.1. Hydrogen pressure performance for pressurized delivery of AB.	47
Figure 5.2. Prototype IV bag reactor.	49
Figure 5.3. Performance of IV reactor at various H ₂ flow rates.	50
Figure 5.4. Sensitivity analysis based on MATLAB modeling.	52
Figure 5.5. Theoretical maximum reaction temperatures.	54
Figure 5.6. Ideal pressure behavior for regulated fill system.	55
Figure 5.7. Hydrogen pressure performance for regulated pressurized delivery of AB.	56
Figure 5.8. Explanation of regulated fill pressure.	57

Figure 5.9. Model of ideally designed 20 gram AB system using hydrogen pressure.	59
Figure 5.10. a) under sized b) ideally sized, 10 gram AB system using single pressurization....	59
Figure 5.11. Repeatable H ₂ flow from ½ inch diameter AB pellets.	61
Figure 5.12. AB pellets with differing lengths and solution height above surface.....	62
Figure 5.13. Extended duration test with excess solution height.....	63
Figure 5.14. Progression of AB pellet testing.....	64
Figure 5.15. 410x SEM imaging of AB pellet before (left) and after (right) acid exposure.	65
Figure 6.1. Mission length vs predicted load for individual soldier.	70

ABSTRACT

This research addresses the issues of electrical energy storage that warfighters in the U.S. military face. A device is presented that combines an on-demand hydrogen reactor with a state of the art proton exchange membrane fuel cell. This thesis focuses on the design criteria and analysis of the chemical hydride reactor. On demand hydrogen release can occur by controlling the hydrolysis reaction of Ammonia Borane (AB). Maleic acid is used to promote rapid release of hydrogen and trap the ammonia released from AB. Reactor designs are categorized as either delivering liquid or solid ammonia borane into an acid filled reactor. In an effort to design as simple of a system as possible, the delivery mechanisms presented do not use electronically powered devices. The primary safety criterion is that the hydrogen does not overly pressurize and meets the consumption rate of the fuel cell. Two liquid delivery architectures are proposed and tested using the assumption that a pressure differential between two chambers will deliver ammonia borane solution into a reactor. Methods of controlling the exposure of solid ammonia borane to a promoter is also presented. Pressed AB pellets were experimentally analyzed in order to characterize the interaction of solid AB in acidic solution. Designs are ranked against each other using system parameters that are applicable to man portable device. Liquid delivery architectures provided a safe and robust method of hydrolysis control. A bag reactor system that met the hydrogen requirements of a fuel cell was developed and tested. When used to compliment a fuel cell and military grade batteries, such a reactor will save weight and volume for extended missions requiring electronic equipment.

1. INTRODUCTION

The 2018 National Defense strategy from the Department of Defense has expressed a need to increase capability in forward force maneuver and posture resilience [1]. Energy demands remain a key factor to the operational capability and effectiveness of forces in contested environments. The Operational Energy strategy from the DoD lists increasing warfighter capability as the number one objective [2]. Military forces rely greatly on warfighters at the squad level to provide sustained, in theater presence. My research is aimed at assisting these warfighters by advancing their technological arsenal.

The DoD is continually adapting to the technologies that are available and required for success in modern warfare. Dismounted soldiers have seen the forefront of these changes as their dependence on technological equipment has increased. Infantry squads in the Army and Marine Corps, and special operation teams are often required to traverse vast terrain on foot while carrying all their required equipment for extended missions. Depending on the specialty of the team, the mission, and the combat environment, these units could be in the field for over 72 hours before a resupply is available. A typical equipment load out must meet the operational needs for the entire duration of the mission, also factoring in back up supplies to account for extended sustainment. The main consumables that must be accounted for are food, water, ammunition and electrical energy. Energy storage, in the form of batteries, sustains essential operational functions such as communications, data processing, and specialized combat equipment. The US Army estimates that each soldier in a 30 man platoon carries on average 13 lbs. of batteries for a 72 hour mission [3]. This value is commonly upward of 20 lbs. for missions requiring fewer people and additional electronic equipment. Special Reconnaissance missions in the army extending up to 11 days have been estimated to require 236 lbs. worth of battery storage, equating to 40 lbs. per individual [4]. Without improvements to energy storage, these loads could continue to rise if the electrical requirements scale up with continued technological advancements [5] [6].

The intent of this project's is to improve a warfighter's energy density by providing a reliable method to charge batteries in the field using modern fuel cell technology. The Naval Enterprise Partnership Teaming with Universities for National Excellence (NEPTUNE) program allotted funding from the Office of Naval Research to Purdue for research in on demand hydrogen systems. The system we propose requires a soldier carried fuel cell and a hydrogen reactor.

Powder reactants will be carried separately, and added with water to the reactor to promote hydrogen release. Ammonia Borane (AB, NH_3BH_3) has been investigated as a hydrogen storage material at the Aerospace Propulsion and Energy Conversion Systems lab at Purdue's Zucrow Laboratories. When I started on this NEPTUNE project, work had been done to prepare highly pure hydrogen through an acid promoted hydrolysis reaction of AB in water.

At the beginning of my time with the project, leadership from the program encouraged teams to prioritize beneficiary discovery in order to clearly identify both the problem and the people that our technology is aimed to help. Through this process, our team learned that a military component that would greatly benefit from improvements to energy dense power is Marine Reconnaissance. These units consist of squads who are often tasked with long duration reconnaissance missions on foot, carrying all their equipment on their back. With communication being a high priority, these marines must carry excess batteries in order to ensure they can meet their mission requirements. A prior Marine Sergeant who served in Afghanistan claimed that the issue of not being able to recharge batteries directly affected their sustainability and was one of the most limiting factors between resupplies along with ammunition. He stated that "*Our solution to the battery problem is to carry more batteries*" [7]. Simply having a reliable method of recharging a battery is attractive to any soldier or marine tasked with like missions. Not only will it reduce the supply chain demand on electronics, but it will also open up storage space for a warfighter to carry other essential consumables. Upon completion of my degree, I will be joining the explosive ordinance disposal (EOD) community in the US Navy. EOD consists of multiple units tasked with rendering safe potentially explosive threats. The extensive robotics, sensors and computers that these units use is another example of a need for more energy dense electrical power storage. Tools such as the TALON bomb robot, X-ray imaging devices and laptop databases are integral components to the EOD mission. Excess batteries are required to ensure that these devices will continue to operate within a safety margin. The proposed two part device (fuel cell and reactor) has potential to operate in a military environment to complement these energy needs.

A primary challenge associated with developing a charging device to an operational level is the control of the hydrolysis reaction within a reactor. Controlling the release of hydrogen allows for a system to operate at lower pressures and temperatures than typical compressed hydrogen or thermally released hydrides. My thesis focuses on presenting and comparing robust reactor

designs that control hydrolysis rates without electronic inputs and are capable of meeting the mission requirements of a combat ready device.

2. BACKGROUND

2.1 Energy Storage in the Field

The BB-2590 Lithium-Ion battery is one of the most widely used power sources for man portable equipment throughout the DoD [4]. Military units use the BB-2590 to power essential communication devices such as the SINCGARS, ASIP and FALCON Radios. It is also used for advanced robotic, surveillance and weapon systems. It stands 4.4 by 2.4 by 5 inches and weighs 3.1 lbs. The rechargeable battery has an energy rating ranging from 225 Wh to 294 Wh for higher capacity models [8], [9]. The aim of this thesis is to present a system that improves on the BB-2590 energy density and provides a method to recharge them in the field. A report from the Center for Army Analysis estimates that using rechargeable batteries instead of disposables reduces the total mission battery load by 45% for direct action (5 day) missions and 71% for special reconnaissance (11 day missions) [10]





The prevailing issue surrounding portable power solutions is that dismounted units currently lack a reliable charging capability when they are detached from the power supplied by a vehicle or generator. Without a method to recharge, extended missions on foot require soldiers to carry their entire electrical power needs, also factoring in emergency reserve requirements, in the form of batteries [11]. Not only do the previously mentioned constraints add excess weight, but once a battery has been used; it effectively becomes dead weight and wasted space in a warfighter's pack until it is disposed of. The issue is highlighted by the fact that lithium ion batteries do not consume products and are therefore the same weight despite their state of charge.

One developed solution for extended dismounted missions is the Solar Portable Alternative Communications Energy System (SPACES) that can accept various sized foldable solar panels to charge any device [12]. Though useful, such a device is limited in practicality due to its dependence on the sun, slow energy output and large visual footprint. There are many military operations where moving at night, and remaining hidden during the day would require an alternate source of energy.

2.2 Fuel Cells

Small-scale fuel cells have been identified as viable portable electrical power generators. Table 1 presents some of the currently tested and developing systems targeted for the dismounted warfighter.

Table 1. Comparison of the different portable fuel cells.

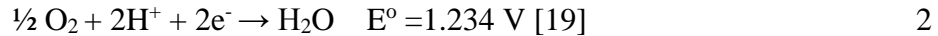
				
System	Ardica 20W: Wearable Power System (WPS) [13], [14]	SFC Energy: Jenny 600S [15]	UltraCell: XX25DMFC [16], [17]	SAFCCell: PP-50-Flex [18]
Fuel Cell Type	PEMFC: Chemical Hydride: Alane (AlH ₃)	Direct Methanol Fuel Cell (DMFC)	Reformed Methanol Fuel Cell (RMFC)	Solid Acid Fuel Cell
Nominal Power [W]	20	25	25	50
System dry weight [kg]	N/A	1.7	3	N/A
System Dimensions [inch]	7x 8x 0.83	7.2x 2.9x 9.9	10.7 x 8.1 x 3.9	N/A
Fuel Cartridge Weight [kg]	.08	0.371	0.620	N/A
Cartridge Dimensions [inch]	N/A	6.5x 2.36x 2.36	9.25x 2.95 x 2.56	N/A
Energy Capacity [Wh]	65	400	440	440
Run Time per Cartridge [hours]	N/A	12-16	18	N/A
Energy Density [Wh/kg] (72 hours @ 20 W)	463	562.6	321.2	648.5
Energy Density [Wh/L] (72 hours @ 20 W)	528	315.6	171	N/A
Start Up Time [min]	Instant	Instant	20	N/A
Orientation Limits	No	Yes	Yes	N/A

*N/A: Not available

Of these systems, the WPS, Jenny 600S and XX25 have been certified and tested in a military environment [14], [4]. The energy densities are for the most part improvements from the 210 Wh/kg and 340 Wh/L of the BB-2590 Battery (high capacity). Though viable, these systems are not without limitations. The methanol fuel cells are both complex systems, limited in operating orientation and requiring hybridization with a battery. Stored methanol, along with alane cartridges, also present a risk if ruptured. While not much data is available on the SAFCcell, solid acid fuel cells tend to emit heat and require a longer start up time [5], [17], [19].

2.2.1 Proton Exchange Membrane Fuel Cell

Of available fuel cell technology, the Proton Exchange Membrane Fuel Cells (PEMFC) have been identified as being promising for a man wearable charging system due to their utilization of oxygen from the air, low heat and sound signatures, non-toxic byproducts and potential for high energy density. These features would allow them to be used near enemy lines in most environments. They can also be easily scaled for a variety of applications requiring on demand power. Equations 1 and 2 represent the anode and cathode reactions that occur on either end of the membrane electrolyte.



For most PEMFCs, the oxygen is easily drawn from air. Unlike a battery, individual fuel cell stacks do not store energy, but rather generate it from the oxidized fuel. Electrical current, heat and water are the only byproducts of a PEMFC. The hydrogen consumption rate is dictated by the size and rated power of a given fuel cell, as well as the power draw from the applied load. In other words, a PEM fuel cell will adjust its hydrogen consumption to match the load that it is powering. Hydrogen flow is typically dead headed to the anode membrane, meaning that as long as there is a positive pressure of pure hydrogen, the stack will be able to meet its current requirements. Such a feature will be key in a reactor design and will be discussed below. Flow rate values will be given in standard liters per minute (sLpm).

Today, PEM fuel cells have efficiencies of 40-60% [4], [19], [20]. Work by companies such as Ballard Power Systems is continuing to optimize fuel cell stacks in order to reduce cost, efficiency and size of portable PEMFCs. Much of these system's feasibility depends on hydrogen storage. PEMFC are highly sensitive to impurities and can easily be damaged from poisonous gasses contacting the membrane. Storing and preparing pure hydrogen fuel becomes a major component in designing a soldier worn fuel cell system.

2.3 Chemical Hydrides and Organic Acids

Hydrogen is a desirable fuel in any application due to its high gravimetric energy density of 120 MJ/kg, but is limited by its low volumetric energy density of 8 MJ/L (for liquid) [20], [21]. The DoE has targeted 6.12 MJ/L for portable hydrogen storage systems [22]. Requiring either cryogenic or pressurized storage to meet this goal, pure hydrogen is not likely a viable solution for mobile devices. Alternative hydrogen storage methods include compounds that either absorb or chemically bind hydrogen. Chemical hydrides show promise for portable hydrogen storage due to their high hydrogen density and on demand hydrogen production. A chemical hydride can typically be dehydrated by the addition of heat (thermolysis) or reaction with water (hydrolysis) [23]. The advantage of releasing hydrogen through hydrolysis is eliminating the high heat or pressure required by metal hydrides or sorbent materials. Ammonia borane (AB, NH_3BH_3) has been identified by researchers as a promising hydride for on board storage. AB holds 19.6 wt.% hydrogen by mass, is relatively stable in aqueous solution and air and can produce non-toxic byproducts from hydrolysis. Stored as a solid white powder, AB has a density of 0.7 g/cm^3 and is soluble in up to 0.351 g/ml [24]–[27]. Figure 1.1 demonstrates the hydrogen density advantages that ammonia borane provides over alternate hydrogen storage methods, including liquid, gaseous, and metal hydride storage.

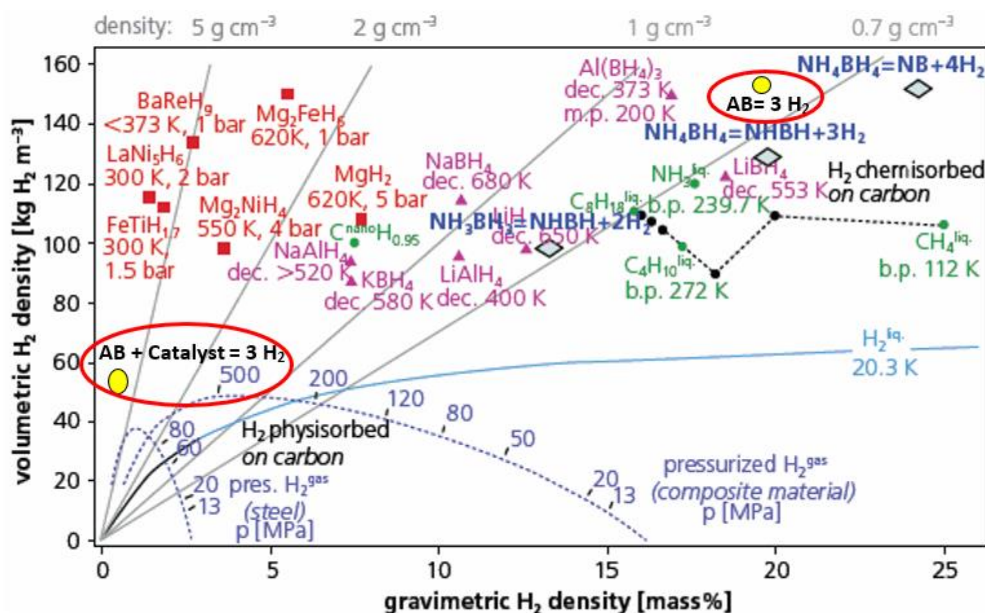
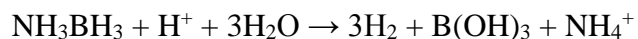


Figure 2.1. Gravimetric and volumetric energy densities for hydrogen storage materials, modified [28].

Circled in red to the upper right is the condition most similar to the release of hydrogen from pure AB. The effect of adding an organic acid catalyst, described in detail below, is circled on the left of the plot. While the catalyzed hydrolysis greatly reduces the reactants energy density, it still has a volumetric energy density preferable to that of compressed hydrogen. The main advantage of AB over all metal hydride and absorptive materials is the stability and low temperature of release. Though water should be accounted for in the overall energy density of the hydrolysis reaction of AB, it is assumed that water is an in-situ resource in a portable application and is not factored into the reactant weight. The overall hydrolysis reaction of AB is summarized in Equation 3, resulting in the release of three equivalence of hydrogen, ammonia, and boric acid.



Without a promoting agent or catalyst, this reaction will take over 80 days for full yield [27]. Previous research at Zucrow has identified organic acids as a low cost, low toxicity and fast kinetic promoter. The most attractive feature of acid promoted hydrolysis is highly pure hydrogen can be discharged when the acid provides a proton to suppress the NH_3 by forming NH_4^+ in solution. In a low pH environment, the overall reaction process will reduce to equation 4.



4

Ammonia release is the primary concern with AB due to its poisoning effect on a PEMFC membrane electrolyte. Ammonia concentrations as low as 30 ppm have demonstrated irreversible damage to the membrane surface. Likewise, carbon monoxide levels exceeding 10 ppm have negative effects as well [29], [30]. Previous work in our group has verified highly pure hydrogen released from equation 4 using Fourier transform infrared spectroscopy (FTIR). The FTIR was used to sample the gas released from AB solution mixed with a catalyst. Testing with organic acids has proven that this reaction mechanism produces less than the lower detection limit for NH_3 (7.4 ppm) and CO (19.3 ppm). Using platinum catalysts instead resulted in up to 1100 ppm of ammonia released. Additional FTIR analysis was performed to prove that acid-promoted hydrolysis will produce pure hydrogen with various water sources, including sea water, cola and synthetic urine [31]. The only significant difference in gas concentration between water sources was carbon dioxide. Even the highest of these values (2500 ppm for Cola) was well below the reported contamination level of 100,000 ppm [29].

Previous studies in our group have screened a wide variety of organic acids for promoted hydrolyses and compared their reaction kinetics. An ideal acid will be low cost, safe to handle and highly soluble in water to reduce the size of a reactor. Additionally, literature has shown that a low pKa value is correlated with rapid kinetics since the hydrolysis reaction is first order with pH [32]. Of the acids considered, maleic acid ($\text{C}_4\text{H}_4\text{O}_4$) was found to be well balanced with these considerations. These studies also demonstrated that 1:1 equivalence of acid was sufficient to fully promote hydrolysis. For the sake of consistency, maleic acid (Sigma Aldrich, Part #: M0375, 99% purity) at a 1:1 equivalence of AB was used for the designing and testing in this research [31].

While other viable chemical hydrides such as sodium borohydride are also capable of hydrolyzed hydrogen discharge, this research focused on designing a system around the properties of AB. With AB selected as the hydrogen precursor, promoted by maleic acid, a robust method of hydrolysis control needed to be designed.

2.4 Design Targets

Initial designs for a portable reactor utilized a spring loaded piston to inject pre mixed AB solution through an orifice into a reaction headspace containing maleic acid solution. The design shown in Figure 2.2 provided some mechanical complications such as O-ring sticking and orifice clogging leading to an unsteady rate of injection. Further iterations have incorporated a peristaltic pump to deliver the solution of AB to the maleic acid reactor.

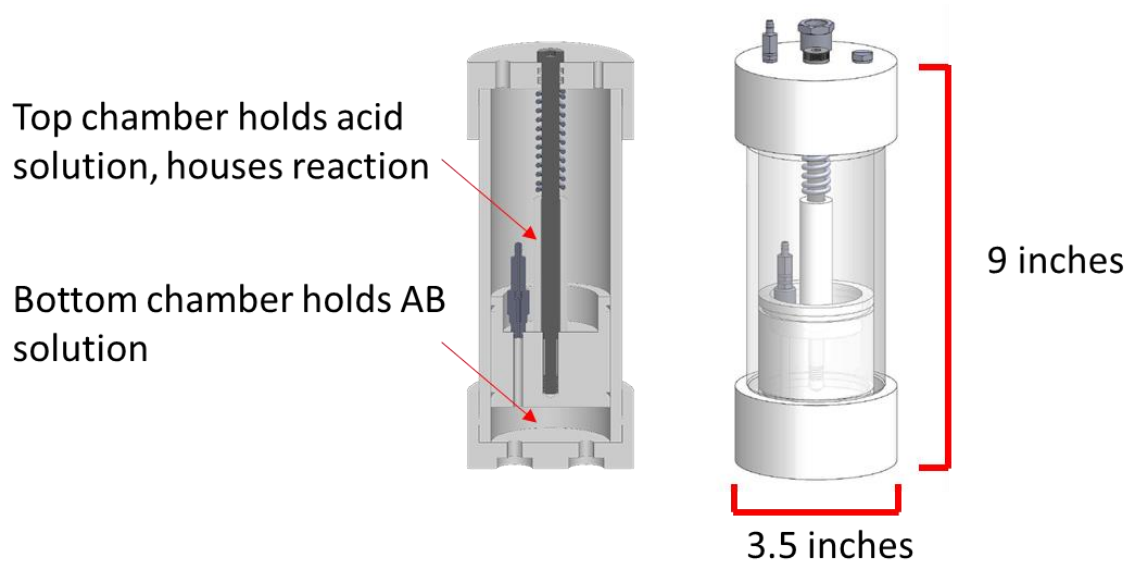


Figure 2.2. AB solution delivered by spring loaded piston.

The cylindrical reactor shown in Figure 2.3 is an acrylic reaction vessel with an internal volume of 150 ml and mass of 180 grams. Three 10-32 to 8th inch hose barb check valve fittings on the lid of the vessel seal the reactor and allow for hydrogen out flow and AB solution in-flow. The peristaltic pump, powered by a 9 V battery, moves solution from the ammonia borane holding vessel into the reactor. A normally closed pressure switch is wired to the pump and will open the circuit if the set pressure is exceeded in the reaction chamber. The system is designed to operate around 22 psia and is capable of holding up to 30 psia of pressure. The reactor is sized to accommodate up to 80 min of target hydrogen flow (about 0.5 sLpm).

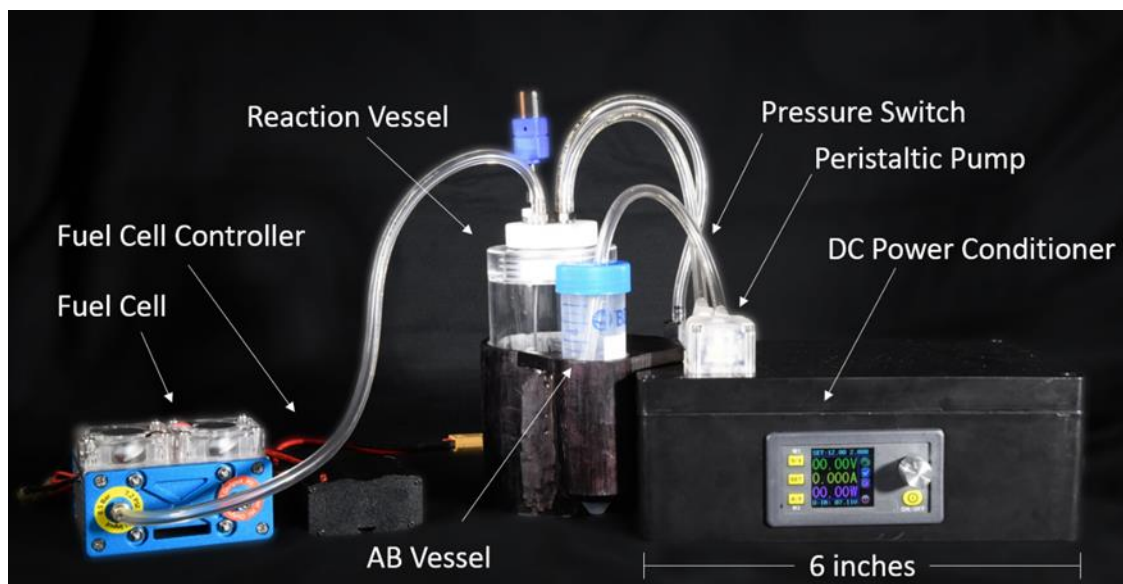


Figure 2.3. AB solution delivered by peristaltic pump.

A focus of this research was to design a system based off the current working reactor but independent of electrical inputs to sustain controlled hydrolysis. The desired outcome is a final system would either be lighter, more robust, less expensive or have an extended operational life. Eliminating a starting battery and motorized delivery system could increase the energy density if the mechanical counterpart consisted of lighter components. Additionally, eliminating the power drawn by the motorized delivery will increase the power output available to charge devices. The robustness of the system could be increased by eliminating the potential drawbacks that dependence on a lithium ion battery could entail, such as impact, temperature and moisture exposure limitations. The total system cost could also be decreased by simplifying the hydrolysis control methodology. Finally, a system free of li-ion batteries could have a shelf-life dependent only on the reactants in storage.

The five overarching go-no-go metrics identified for the system are outlined in Table 2.

Table 2. Go-no-go metrics for system.

Metric	Description
No electrical input	Premise of research: Extend life expectancy of reactor by eliminating lithium ion batteries
Start/Stop at anytime	In order to be used in the field, the reaction must be easily initiated and stopped at any point
Emergency pressure relief	At any location in the system, over-pressurization must be relieved in a safe, non-destructive manner
Hydrolysis Control	Hydrolysis must be able to meet the fuel cell consumption rates at any given electrical load
System energy density	In order to meet goals of the project, the energy density of the system must exceed that of a BB-2590
Safety	Stay below hydrogen pressure and solution temperature limits

As mentioned above, the charger's purpose is to accommodate currently used batteries. The Revision Military's *Squad Power Manager* (Model #: SPM-622) has been identified as complimentary device to be used with the charger for field testing and use. An intelligent power manager has the capability to harvest and condition power from a wide variety of inputs to charge all electrical systems carried by a soldier [33]. The SPM-622 is currently used in active EOD and infantry squads in all branches of the US DoD. The manager weighs 1.0 lb., has dimensions of 1.2 by 4.4 by 3.2 inches and is capable of receiving a max current of 10 Amps from a range of 4 to 34 VDC [34]. A smaller scale version is also available for individual applications and weighs 0.3 lbs. The SPM-622 shown in Figure 2.4 has been tested in the lab and has proven compatible with the pump controlled reactor and a commercial PEM fuel cell.



Figure 2.4. SPM-622 harvesting power to charge military equipment. [34]

2.4.1 DoD Standards

Certified field ready equipment must pass specific tests described in military performance and standard documents. MIL-STD-810 details the environmental factors that a system should be tested to endure [35]. MIL-PRF-32383 specifies the exact testing that must be done on a BB-2590 battery to mimic what it may experience in operation. Table 3 presents the environmental stresses and performance tests that the battery must pass in order to be certified for use.

Table 3. BB-2590 Performance Evaluation [36].

MIL-PRF-32383 (2590 Performance Assessment)	
Specifications	Test/Validation
Extreme temperature operation	Stored 4 hours and discharged at both -30°C (-22°F) and 55°C (140°F)
Altitude	Perform at simulated pressure for 50,000 ft
Thermal shock	Operate in a range from 75°C (167°F) to -59°C (-75°F) for greater than 2 hours
Mechanical shock	Shock mounted battery with no less than 40g with a pulse duration no less than 18 milliseconds
Vibration	Batteries shall be capable of withstanding vibration environments without sustaining physical or electrical damage. Batteries shall exhibit no voltage fluctuations during vibration
Water Immersion	Operation after submersion in 33 ft in salt water for greater than 5 min and 3 ft for 2 hours
Transit drop	Dropped at varying angles from no less than 30 inches onto concrete
Battery storage life	Storage for 622 hours (approximately 26 days)
Nail penetration	Shall not burn or explode after 2.5 mm DIA stainless steel nail into cell
Crush	Shall not react violently, burn or explode when crushed
Projectile from exposure to flame	Shall not produce shrapnel when subject to flame

While a hydrogen reactor has fundamental differences to a lithium ion battery, the same metrics can be used to determine if a portable system is comparable to its battery counterpart. These environmental considerations acted as a framework from which a feasible design could be presented. It should be noted that an end system fuel cell will also have to be assessed in the same manner and may influence the final system's performance. In addition, unlike a 2590 battery, the reactor must be considered for both an in use and under storage states. Depending on regulating operation procedures, some performance tests may be more lenient for the reactor in operation. For example, water immersion tests may only be necessary for the storage configuration, not under operation since the reactor will not be used under water.

It should be noted that while robust in design, the BB-2590 does pose a risk in the event of battery failure. Failure of lithium-ion batteries can lead to the rapid release heat and corrosive chemicals [37]. An attractive feature of a fuel-cell/reactor system is that the consequence of failure could be reduced. While highly flammable, hydrogen gas is nontoxic and relatively low explosive potential in such a small volume due to its low volumetric energy density. A primary design consideration was eliminating any compressed mixture of air and hydrogen. The risk of explosion or an air-hydrogen mixture was assessed as a metric of safety for each design.

3. REACTOR DESIGNS

3.1 Preliminary Designs

The considerations described in Chapter 2 are a framework from which feasible reactor designs were developed. One of the driving design parameters was to ensure that all ammonia would be captured by the organic acid trap. Expanding equation 4 from section 2.3 gives the chemical process of acid promoted hydrolysis.



Equation 6 will favor the left reactants at lower pH and induce NH_3 capture. For this reason, reactor designs require exposure of either aqueous or solid ammonia borane to an acidic environment. Potential design architectures were categorized by either solution or solid addition of AB to the acidic solution. All designs consist of a main reactor vessel/chamber that houses the reaction and produces hydrogen. Each architecture also has a fuel housing and delivery mechanism that accounts for the AB before it is hydrolyzed. The fuel housing is either in the main reactor vessel, as is the case for most solid AB designs, or it is an entirely separate vessel, referred to as the AB delivery vessel. The following figure shows the flow of concepts for a hydrolysis management scheme starting with the assumption that hydrolysis will be controlled without electric inputs. Section 3.1.1 discusses the liquid mixing designs shown on the left of Figure 3.1. These concepts are divided into either pressure dependent mixing or constant rate mixing. Section 3.1.2 discusses all of the designs using solid AB which are shown on the right of Figure 3.1. These concepts consider either controlled delivery of solid AB or the controlled exposure of this AB to acid inside a reactor.

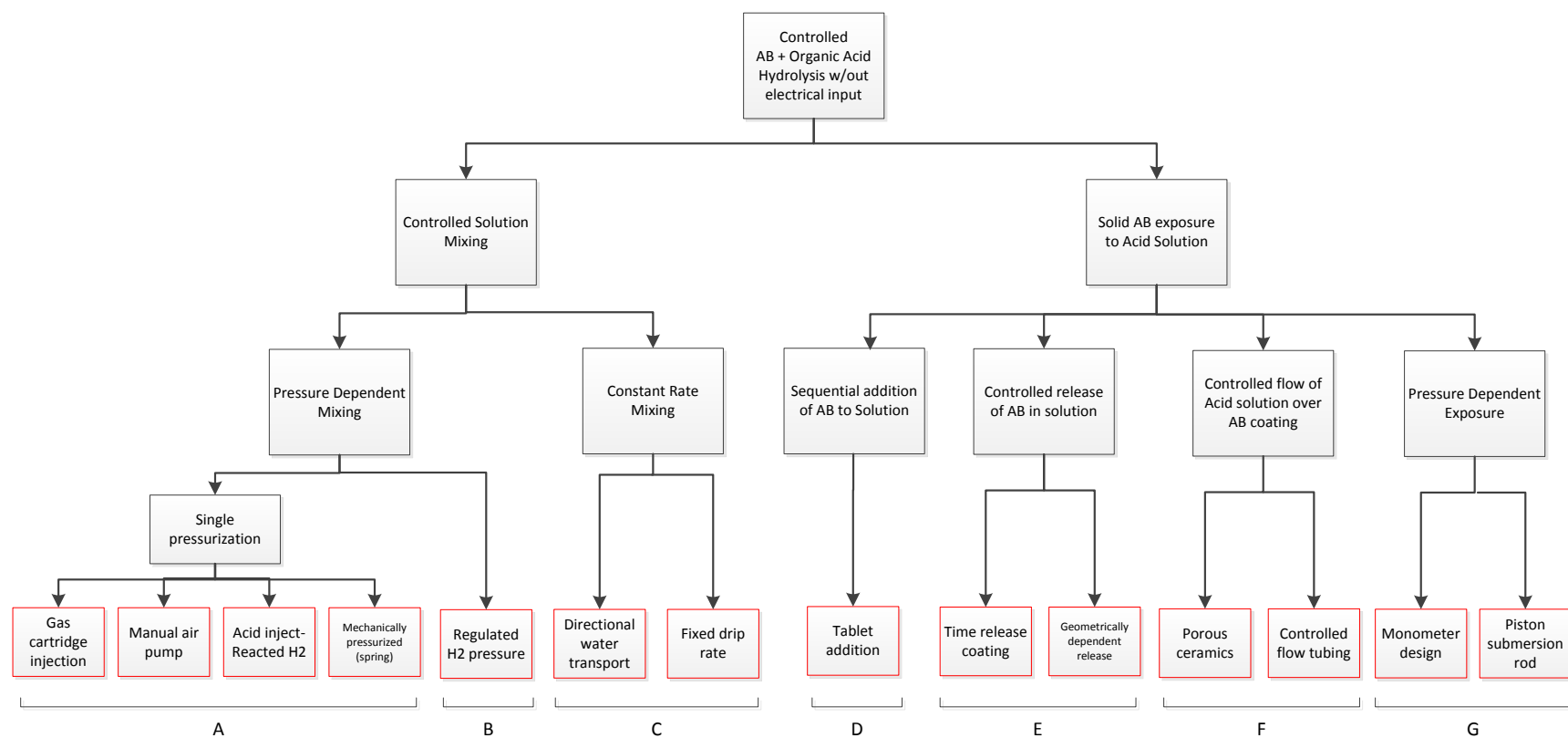


Figure 3.1. Design breakdown based on hydrolysis control method.

3.1.1 Liquid Mixing

Thoroughly mixed AB solution can be added to a reactor containing a solution of organic acid at a controlled rate to directly regulate how much hydrogen is produced. Various delivery methods of the AB solution are discussed here. One method of control is setting a fixed drip or permeation rate for one or both solutions (design C in Figure 3.1. Design breakdown based on hydrolysis control method). A unidirectional permeable membrane or a constant drip injection could be used to deliver AB solution at a constant rate correlating to a constant generation of hydrogen. The main dilemma stems from the fact that the rate of hydrogen consumption is associated with the electrical load put on a fuel cell. A constant reaction rate is less desired than a rate that adjusts with the hydrogen demand. One way to accommodate for this variable demand is by having the solution addition depend on the pressure in the reaction chamber. Hydrogen gas will pressurize the sealed reaction vessel if the consumption rate required by the fuel cell is lower than the hydrolysis rate. The rise in pressure can be used to indicate that AB addition can be slowed or stopped. Using a check valve allows ammonia borane addition to depend on the pressure differential between the AB solution and the reactor chamber. Additionally, a check valve sufficiently seals the reaction chamber to prevent pressurized hydrogen from escaping. An orifice can be put in line upstream of the check valve to achieve a set drip rate. An externally applied pressure must be applied to the AB solution to promote flow.

One method is to pressurize a sealed headspace above the AB solution with gas. The gas can be delivered from either air pumped in, inert gas from a stored cylinder, or hydrogen released from hydrolysis. A depiction of this design, denoted A, is shown in Figure 3.2. Such a design requires two pressure holding vessels. Also shown in Figure 3.2 is design B. Design B depends on the same fundamentals to deliver AB solution as the A designs, however, a regulated hydrogen line can be used to re-fill the headspace in the delivery vessel using any excess hydrogen in the reactor. The end goal of a regulated pressure design would be a controlled cycle at a steady state operating pressure. If a steady pressure is achieved, the system should sustain itself for the entire length of the reaction. Unlike a single pressurization, it would not be limited by the upper chamber pressure decay associated with a single fill of gas.

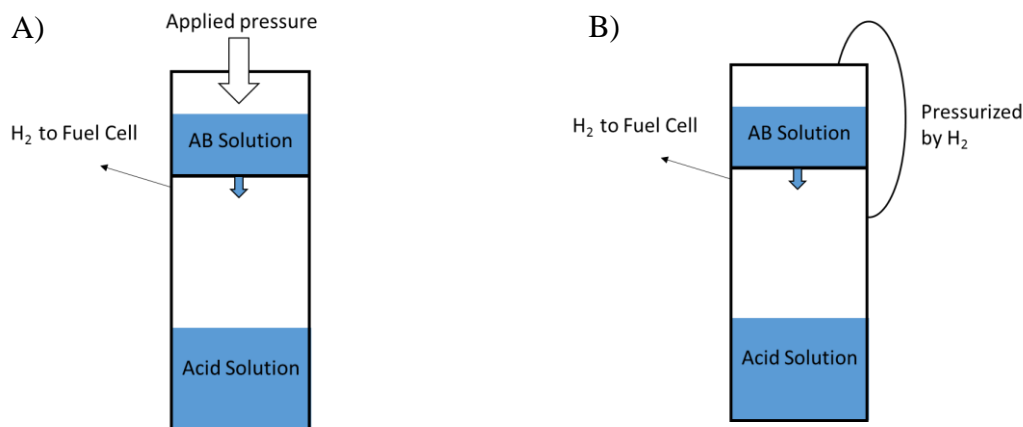


Figure 3.2. A) Externally driven AB solution to reactor; B) Pressurized delivery of AB solution from reactor hydrogen.

One of the advantages that both these architectures provide is the mixing benefits of having both ammonia borane and the acid promoter fully dissolved in solution. Once AB is dropped into solution it will immediately come into contact with the promoter. Bubbling that occurs due to hydrolysis also aids in reaction circulation and mixing. Another advantage of two vessel designs is that the risk of expulsion is reduced since the fuel is stored separately.

3.1.2 Solid AB

My research also looked into controlled hydrolysis of solid AB in an aqueous acid solution as depicted on the right side of Figure 3.1. The primary advantage that most solid fuel storage designs provide is the simplicity of having a single reactor vessel. Solid AB is appealing for use in the field because it also does not require an added step of mixing another solution. Like liquid droplets, dry AB in either the powder or pressed form could be sequentially added into a reactor or exposed to the acid at a controlled rate (design D). Sequential addition of AB into the reactor was ruled out because of the design challenge of sealing the delivery port into the reactor since a fluid flow check valve could not be used. Early designs for this project looked at dispensing pellets into the reactor at a controlled rate, but issues arose in preventing acid from interfering with the delivery mechanism at a non-upright orientation. Instead, methods of controlled release of ammonia borane as a solid submerged in acidic solution were considered (design E). These designs were categorized as either being controlled by dissolvable coatings such as those used with pharmaceutical time release capsules or by adjusting the surface area geometry exposed to the acid,

much like a hybrid rocket grain. Similarly, a catalyst bed like reactor has been proposed by flowing acid solution through an AB coated surface (design F). A surface could be designed in such a way to control the rate at which the acid seeped through to contact the AB. Ceramic monolith materials with porous channels such as cordierite was suggested as a means to hold a coating of AB and control the rate of solution permeation. Such honeycomb materials have been experimented in literature as flow through catalysts for Sodium Borohydride reactors [38]–[40]. Both designs E and F are depicted in Figure 3.3.

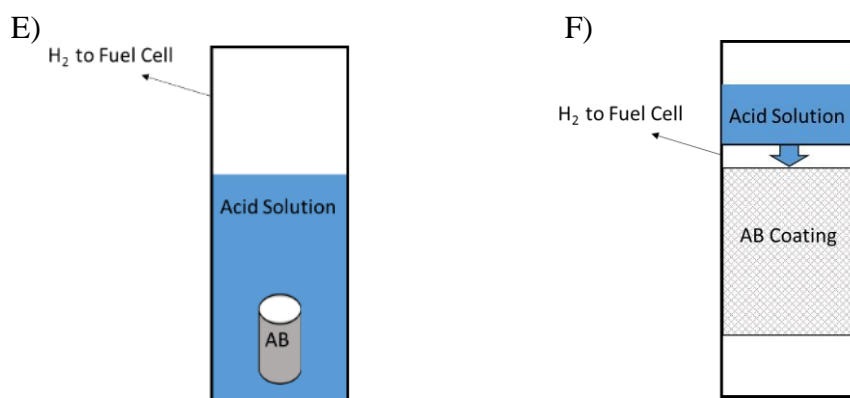


Figure 3.3. E) Controlled release of AB in solution; F) Controlled exposure of AB to solution.

AB has demonstrated promising storability and reaction efficiency in pressed pellet form. Literature reviews have identified methods of impregnating surfaces with ammonia borane using either Tetrahydrofuran (THF) or methanol solution [41], [42]. Coated or pressed AB could provide a sturdy method of storage as well as reliable hydrogen release. These solid hydrolysis designs discussed fall under the same restrictions as design C; and that is that a constant rate is not necessarily a controlled rate. Because of this, a practical design, capable of meeting the metrics in Table 2, must be pressure dependent. Design G represents all architectures in which solid AB is removed from contact from the acid at a given maximum pressure. A system designed in this way could either utilize a pellet or coated surface. One method to extract the AB coated sample from solution would be using a piston cylinder that is backed by a spring. Sizing the piston head, coefficient of friction and spring coefficient can allow the volume of the cylinder to expand at a selected pressure. The piston head movement can be used to either pull the AB out of solution from above, or lower the solution height below the AB. The pressure dependent exposure concept is depicted below in Figure 3.4. G) Pressure dependent exposure of AB to acidic solution. Figure 3.4.

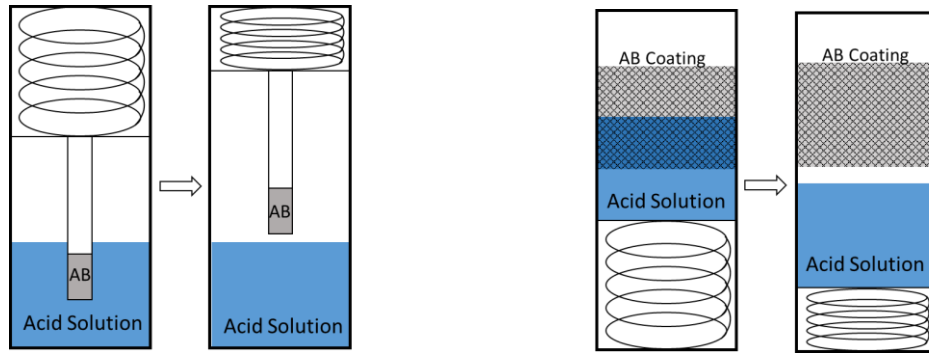


Figure 3.4. G) Pressure dependent exposure of AB to acidic solution.

3.1.3 Design Down Selection

Of the designs presented in Figure 3.1. Design breakdown based on hydrolysis control method., only pressure dependent hydrolysis mechanisms (designs A, B and G) were considered viable for a portable application. All other designs (C, D, E and F) would provide a constant or pre-set hydrogen release rate and would require either a buffering or venting mechanism in order to accommodate to the changing consumption rates of a fuel cell. While feasible for other applications, storing or venting hydrogen in a man worn system was determined to negatively affect safety and efficiency considerations. Designs E and F were still assessed in an trade study in order to compare to each other; they are labeled in red in Table 4 and Table 6.

3.2 Energy Density Assessment

An overall energy density assessment was performed based on the DoE's target for portable energy systems. Next an energy density assessment compared the potential of each design. For the sake of simplified comparison, gravimetric energy densities were compared for each system since the change in volumes was assumed negligible.

3.2.1 Overall Energy Density Goal

A full high capacity BB-2590 battery is rated for 294 Watt hours which equates to 8.8 grams of hydrogen gas using the accepted energy density of 120 kJ/g of hydrogen [9], [21]. Equation 4

gives that 8.8 grams of hydrogen can be achieved with 45 grams of AB assuming an ideal system (no losses). Applying a standard fuel cell efficiency of 50% to the same calculations would require 17.6 grams of hydrogen and 90 grams AB. For a full equivalence of acid, 337 grams of maleic acid would be required. Assuming that water is not factored in as part of the system weight, the system reactants alone give 40 g_{H2}/kg_{reactant}. The DoE has targeted 30 g_{H2}/kg_{system} for rechargeable hydrogen storage systems [22]. This value will be used to determine the amount of additional hardware that can be allotted to a system. Equation 8 provides the allotted mass of a system given the energy density of the reactants and the target value for the system as a whole.

$$\frac{40 \text{ g H}_2}{1 \text{ kg reactants} + h \text{ g hardware}} = \frac{30 \text{ g H}_2}{1 \text{ kg system}} \quad 8$$

$$h = \frac{330 \text{ g}}{1 \text{ kg reactants}}$$

The value h provides the mass of hardware that can be allowed for every kilogram of reactant to match the energy density target of the DoE.

For an end system reactor to be compared to a 2590 battery, the weight of a fuel cell and any other complimentary devices such as the SPM-622 must be factored in. The energy density of a 2590 battery is equivalent to 13 g_{H2}/kg_{system}. Targeting this value, the overall h value for a fuel cell/reactor system is 2080 g/kg_{reactant}.

3.2.2 Energy Density Comparison

To evaluate and compare potential energy densities, the AB reactor from Figure 2.3 was used as the base design. Each model was analyzed at the power output equating to 1 kg of reactants while maintaining reactor vessel masses. M in equation 9 denotes the added masses associated with each reactor architecture.

$$\text{Energy Density} = \frac{40 \text{ g H}_2}{1000 \text{ g reactants} + 180 \text{ g cylinder} + M \text{ g}} \quad 9$$

$$M = \text{delivery/containment components [g]}$$

The M value, when compared to the target value of h given in equation 8, can be up to 150 grams for the system to achieve its target energy density. The following table shows values for M and energy densities for the evaluated models.

Table 4. Energy density prediction.

Design	Component	mass [g]	M [g]	$\text{g}_{\text{H}_2}/\text{kg}_{\text{system}}$	$\text{J}/\text{kg}_{\text{system}}$
Original	Peristaltic pump	210	368.75	25.8	3.1
	Battery (9 V)	45			
	Pressure switch	90			
	AB solution container	12.75			
	Check Valve	7			
	Tubes/fittings	4			
A (air pump)	Hand pump	60	122	30.7	3.7
	Iv bag	21			
	Pressure cuff	31			
	Check Valve	7			
	Tubes/fittings	3			
B	Regulator	25	144	30.2	3.6
	AB chamber	100*			
	Check Valve x 2	14			
	Tubes/fittings	5			
E	Coating/Binder (50 wt.% AB)	205*	205	28.9	3.5
F	Coated Monolith (15 wt. % AB)	1366*	1366	15.7	1.9
G (piston/spring)	Spring	45	332	26.5	3.2
	Piston/shaft	287			

*Estimated values: all other values were weighed

The components for the original design depicted in Figure 2.3 were weighed in the lab. The peristaltic pump and battery were oversized for this system, meaning that this mass could be reduced. The components used for both A and B designs are described in detail in section 4.2.2. All solution delivery components consisted of Beswick fittings and 1/8th inch PVC flex tubing. The check valves used were 0.5 psi cracking pressure duckbill check valves (Beswick Part #: PRD-2N1-0-3) and the regulator was a miniature single stage diaphragm regulator (Beswick Part #: PRD-2N1-0-3). The AB chamber for design B was estimated since the one experimentally used was stainless steel and largely oversized. The estimate of 100 grams was based off of the 180 grams of the acrylic reaction vessel. Weight estimates for design E coatings were based on

experimental averages of the weights of epoxy casings (described in section 4.2.2). Catalyst coated monoliths are typically capable of retaining 15 to 20 wt.% catalyst. [38] [43]. Figure 3.5 compares the expected hydrogen densities from Table 4 to the DoE target and equivalent density of a 2590 battery.

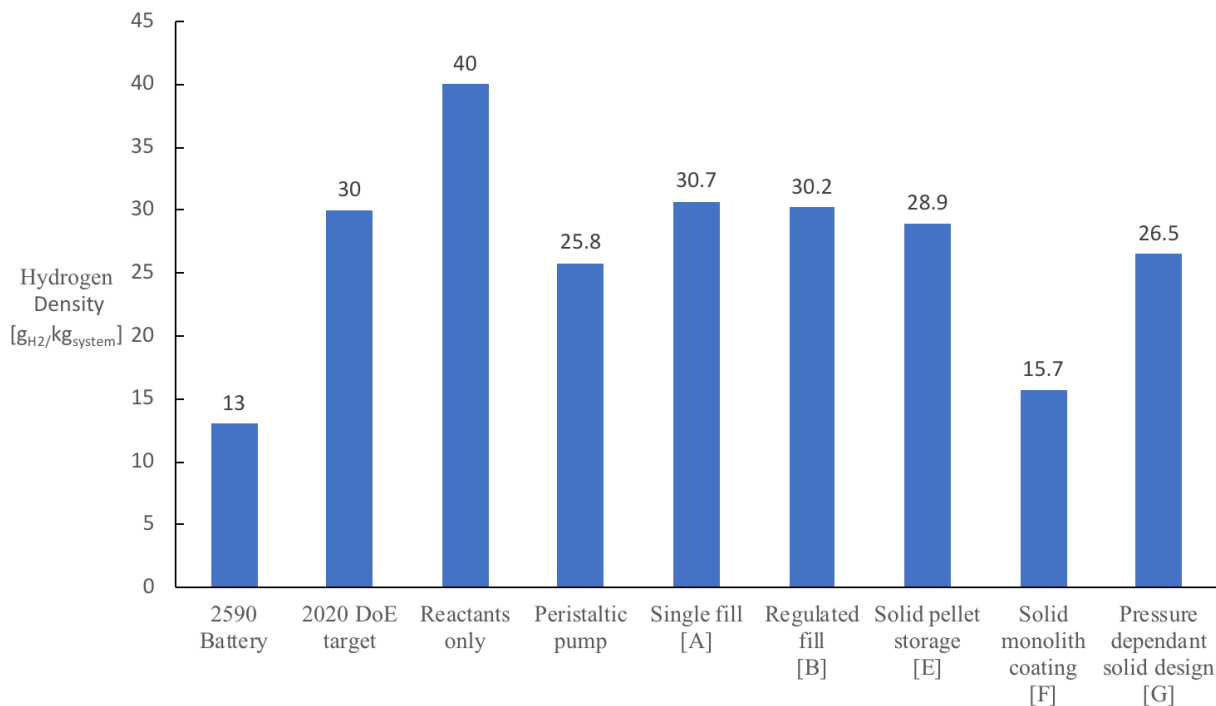


Figure 3.5. Hydrogen density assessment.

3.3 Conceptual Design Trade Study

Apart from energy density, other measurable parameters were identified for a soldier worn system. The following table describes the key factors that would be of consideration in designing a reactor utilized by military personnel. These values were verified by active duty service members with experience in the field. A list of parameters were given to Marine Corps and Navy EOD personnel to weigh on a scale from 1 to 3. Low priority parameters were given a weight of 1 while high priority parameters were given a weight of 3. This small weight range was used in an effort to avoid over-weighting one criterion. The averages were compiled in Table 5.

Table 5. Design parameter weighting.

	Parameter	Description	Weight
1	Robustness	Durability in storage and operation against: temperature, pressure, moisture, agitation	3
2	Energy density	See Table 4.	3
3	Safety	Predicted risk of run-away reaction or human error	3
4	Reactor storage	Reactor stability in storage	3
5	Reactant storage	AB/acid stability in storage	2.5
6	Autonomy after initiation	Is the reaction autonomous after initiation or does a user have to monitor the system?	2
7	Refill procedure	Time and complexity associated with refilling reactants	2
8	Set-up procedure	Time and complexity associated with set up	1.5
9	Take down procedure	Time and complexity associated with clean up	1.5
10	Orientation for operation	What orientation limits does the model have? Will the charger work in a backpack, or must it be set on flat ground?	1.5
11	Production/Cost	Cost of materials/production for model	1

In order to compare expected design performance, a Pugh Chart was set up using these weighted parameters and ranking each system on a scale of -3 to 3 in respect to a baseline value.

Table 6. Preliminary Pugh Chart analysis.

			Peristaltic Pump	Single Pressurization	Regulated H ₂ flow	Controlled Release Pellets	Monolith Catalyst Bed	Pressure dependent exposure
	Property	Weight		A	B	E	F	G
1	Robustness	3	D	2	-1	2	2	1
2	Energy density	3		2	1	1	-3	0
3	Safety	3		0	-1	-2	0	-1
4	Reactor storage	3	A	0	0	2	2	1
5	Reactant storage	2.5	T	0	0	1	-1	1
6	Autonomy after initiation	2		-2	0	0	0	0
7	Refill procedure	2	U	0	-1	2	-1	2
8	Set-up procedure	1.5	M	0	-1	3	2	2
9	Take down procedure	1.5		0	0	2	2	2
10	Orientation for operation	1.5		1	0	3	-1	-2
11	Production/Cost	1		2	1	0	-2	0
	Rated as: (-3, -2, -1, 0, 1, 2, 3)	Total	0	11.5	-5.5	27.5	1	12.5

The peristaltic pump design was set as the datum from which to compare the properties of the other models. Ratings were assigned based on preliminary design assumptions. Of the two liquid mixing architectures (A and B), model A provides greater benefits with a score of 11.5 above the datum. This is due to the fact that model B requires pressurized hydrogen in the delivery vessel; this poses either an increased risk of mixing hydrogen with air or an extended setup procedure. Comparing models E and F shows that a controlled exposure of solid AB outweighs the catalyst bed designs because of the simplicity of reactant storage. A fully coated monolith cartridge adds weight and volume to each individual charge. Model G was incorporated to represent the feasible implementation of solid AB hydrolysis and was ranked the highest among feasible designs with a score of 12.5. Close behind this score is the single pressurization system, with 11.5 points. It was determined that experimental testing would help to clarify any assumptions that were made in the trade study analysis and aid in selecting a finalized reactor design.

3.3.1 Model Selection

While A outranked B in table 6, the regulated flow of hydrogen does provide a potential benefit of having a self-sustained system, and could be applicable in other situations. System level testing was performed for models A and B. No prototype systems for solid AB hydrolysis were designed. Instead, a series of tests were performed in order to characterize the behavior of solid ammonia borane exposed to acidic solution. These preliminary tests would provide essential data for designing any of the solid-state models presented above.

4. METHODOLOGY

4.1 Ammonia Borane Synthesis

The AB used for testing was synthesized in the laboratory adhering to a method developed by Ramachandran and Kulkarni [44]. The method summarized here was used because it was both cost effective compared to purchasing AB and had proven reliability in our laboratory. All reactions were performed in a fume hood due to the release of hydrogen. One equivalent of sodium borohydride (NaBH_4 , Sigma Aldrich, Part #: 213462, 99% purity) was added to a round bottom flask containing a mixing slurry of two equivalence ammonium sulfate ($((\text{Na}_4)_2\text{SO}_4)_2$, Oakwood Chemical, Part #: 099728, 99% purity) in 400 ml of Tetrahydrofuran (THF). The round bottom flask rested in an ice bath to keep reaction temperatures down and sat on top of a stir plate. Individual batches utilized half a mole or 18.9 grams of NaBH_4 . Half an equivalence of deionized water (4.5 ml) was added to the mixture, initiating hydrolysis of the sodium borohydride. The solution was left stirring overnight to ensure all NaBH_4 has reacted. A vacuum pulled filtration system was set up using a vacuum pump attached to a filter flask. A Buchner funnel was packed with about half an inch of Celite and covered by filter paper, the flask was then positioned on the joint neck flask. The THF solution was poured entirely into the filter flask. Occasional rinses of the round bottom flask using THF were used to deliver all reactants into the filter flask shown in Figure 4.1.

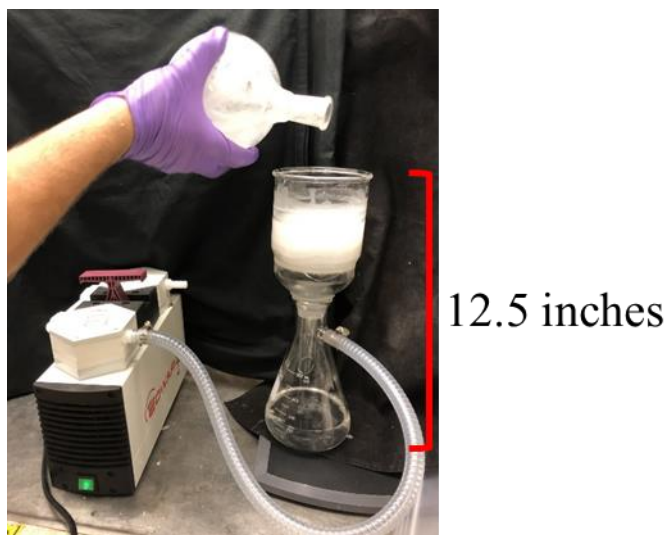


Figure 4.1. Ammonia Borane Filtration.

Proper filtration would yield a completely clear THF solution in which only AB was dissolved. Next, the solution was poured into another round bottom flask that was placed into a heated bath and attached to a Buchi R-215 rotary evaporator shown in Figure 4.2.



Figure 4.2. THF evaporation.

The evaporator was left running until the ammonia borane visibly solidified on the side walls of the flask. The solid AB was then scraped off the walls and left under vacuum to continue evaporating any remaining THF. Finally, the AB powder was delivered into a crucible to be ground to a fine powder. Purity tests were then conducted on the AB samples by comparing the theoretical to actual yield of gas measured in a burette. Typical purity usually gave anywhere from 95% to 100% pure AB. The test for purity based on the volume of gas released relied on the assumption that hydrogen was the sole byproduct and all ammonia was sequestered. Gas composition sampling using the FTIR could be another technique of verifying AB purity. Dry AB batches were then stored in sealed containers under air.

4.2 Reactor Experimentation Setup

4.2.1 Test Stand

All system level hydrogen reactors were tested using a data acquisition system that acquired pressure, hydrogen mass flow, and temperature data from the reaction. Two Unik 5000 Pressure Transducers (0.2% full scale accuracy, 0-50 psia range, Druck, LLC. part number PMP50E6-TB-A1-CA-H0-PE) provided pressure readings for both cylinders and a T-type thermocouple (1.6 mm x 152.4 mm, $\pm 2^{\circ}\text{C}$ accuracy, Omega part number TMQSS-062G-6) gave temperature readings from within the reactor solution. The reactant gas would pass through the equipment stand flowing through a 40 psia relief valve, an air filter, an Alicat M-Series mass flow meter, (accurate to $\pm 0.01 \text{ SLPM} \pm 0.8\%$ of reading, Alicat Scientific part number M-5SLPM-D/5M) and an Alicat flow controller (accurate to $\pm 0.01 \text{ SLPM} \pm 0.8\%$ of reading, Alicat Scientific part number MS-5SLPM-D) to mimic the hydrogen consumption of a fuel cell. The test stand plumbing and instrumentation diagram is given in Figure 4.3.

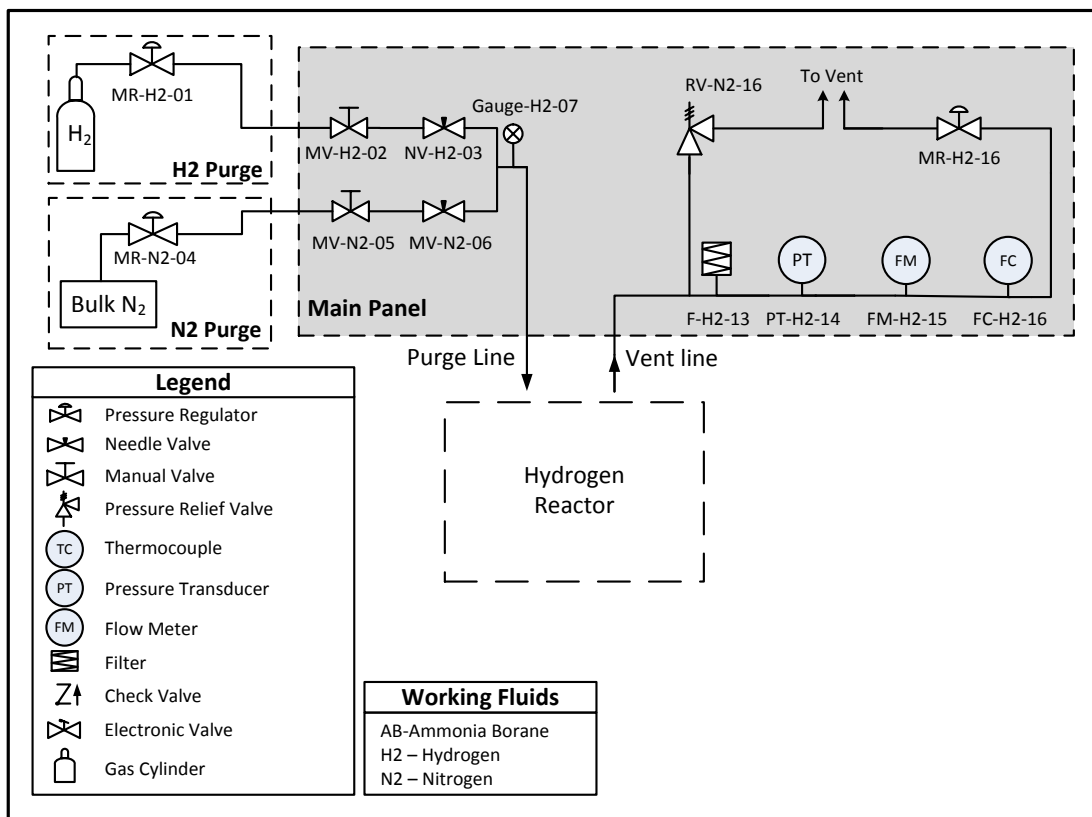


Figure 4.3. Test stand plumbing and instrumentation diagram.

4.2.2 System Design and Procedures

Prior to testing, reaction vessels were purged with nitrogen to remove air from reactor headspace. Bottled hydrogen (Indiana Oxygen, Part #: 181279, 99.999% pure) was then flowed through the system and stand to calibrate the flow meter. For solution mixing system tests, both the AB and acid solutions were thoroughly stirred and injected into their respective containers before the purging using syringes.

Tests performed with the externally pressurized design initially utilized a variable volume, cylindrical reaction vessel to house the acid solution. A medical grade 500 ml intravenous (IV) pressure infuser cuff was used to pressurize a 300 ml PVC IV bag containing the AB solution. The pressure cuff was intended to operate between pressures 5 and 8 psig. The hand pump provided both a pressure gauge and a relief valve in order to keep the cuff within its operating pressure. A plumbing diagram for the infuser delivered setup is given in Figure 4.4.

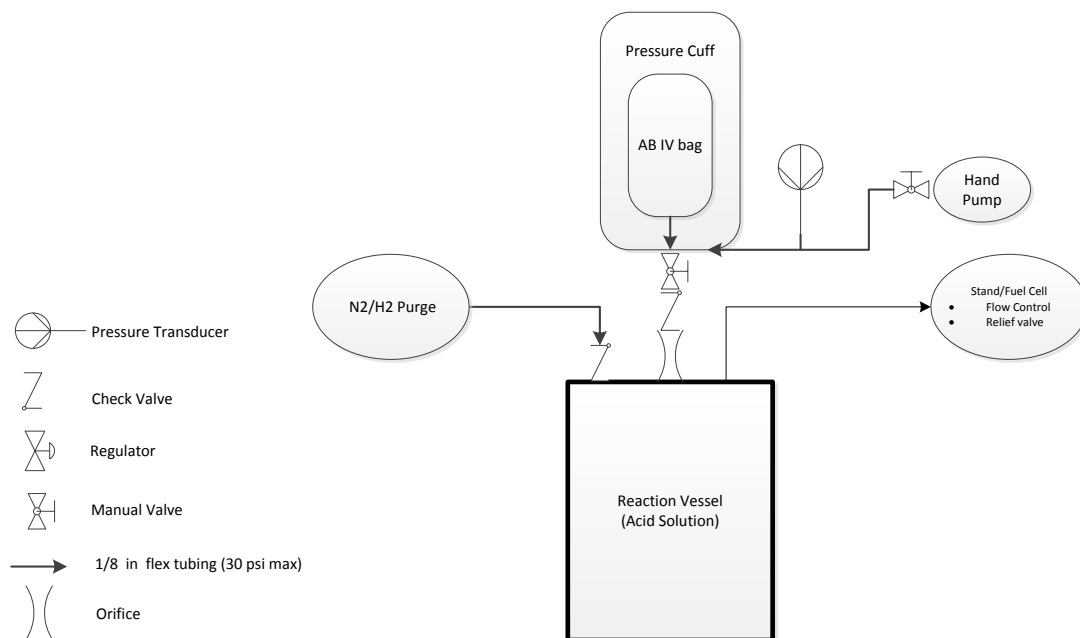


Figure 4.4. Plumbing and instrumentation diagram for A design.

Initiating the pressure cuff tests began with opening the manual valve below the AB IV bag. Next the pressure cuff would be manually pumped to the desired operating pressure.

For tests with design B, the same reactor was used. Two sample cylinders (150 and 50 ml) were used to contain the AB solution and hydrogen gas. A Swagelok cross on the top of the sample

cylinder attached a pressure transducer, vacuum pump, and hydrogen regulator to the upper vessel. Figure 4.5 depicts the test setup used to test design B.

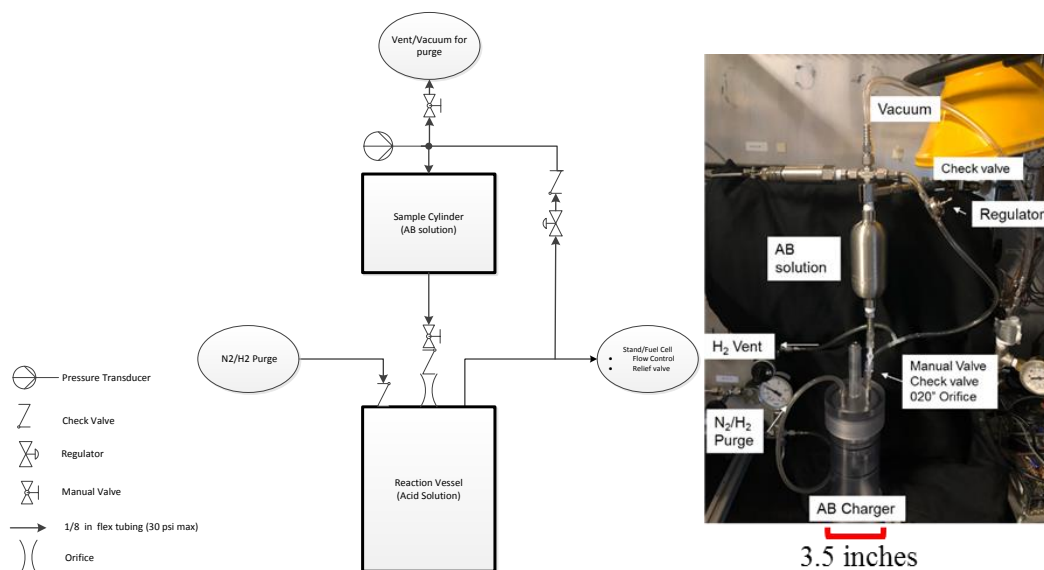


Figure 4.5. Plumbing and instrumentation diagram for B design.

To avoid a pressurized mixture of air and hydrogen, the upper vessel was cycled through an evacuation and nitrogen purge prior to testing. During the system hydrogen purge, the entire system was allowed to pressurize to the desired initial delivery pressure. Once the reaction chamber returned to ambient pressure, the manual valve would be opened and AB would begin to flow to the reactor. In order to achieve a steady pressure trace, both vessel volumes and regulator set pressure were adjusted depending on the amount of reactants used.

Testing with solid AB focused on characterizing hydrogen flow rate with exposed surface area of pressed pellets. AB was pressed into a 0.5 inch dye under 2000-2500 pisa. Pellets were then coated with a clear, inert epoxy (Gorilla Epoxy, composition: bisphenol A-epichlorohydrin polymer) and allowed to cure for 24 hours. A sample pellet is shown in Figure 4.6.



Figure 4.6. Pressed AB pellet.

The epoxy used was both stable with AB and did not decompose in the acidic solution. The same test stand was utilized for all pellet testing, but the flow controller was left open to avoid pressurization. The unrestricted hydrogen flow out of the reactor was recorded by the flow meter. Acid solution was mixed and filled to a specific height in the reactor. The reactor chamber lid used contained a shaft sealed by two O-rings. The pellet was attached to the bottom of the shaft at the desired orientation and the lid was placed onto the reactor. After a nitrogen and hydrogen purge, the shaft was pushed down into the solution, initiating hydrolysis. Figure 4.7 displays the setup for pellet tests.

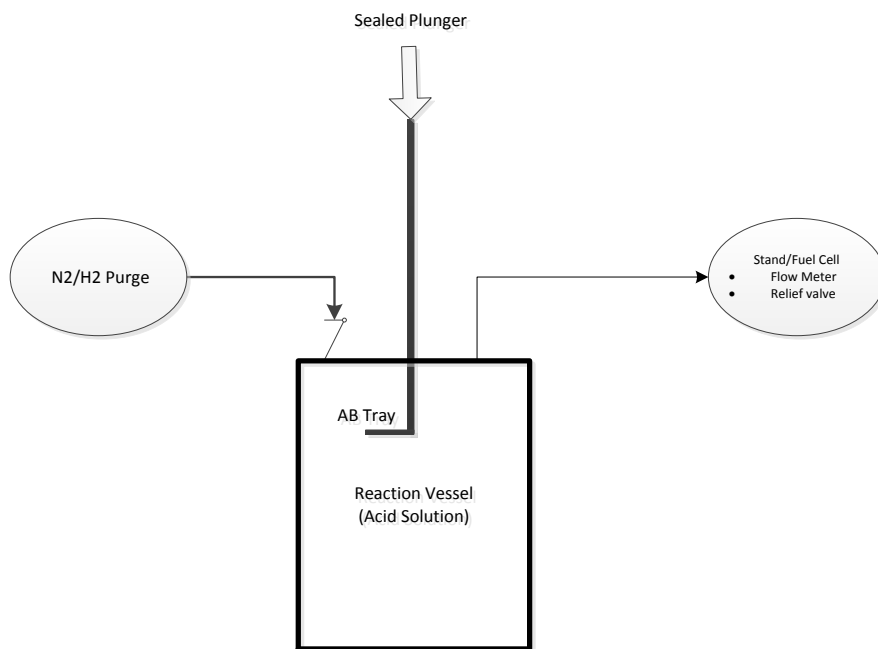


Figure 4.7. Plumbing and instrumentation diagram for AB pellet design.

4.3 Modeling Performance

For both liquid mixing designs, MATLAB scripts were written to predict the nominal pressure performance at a selected size assuming nearly instant hydrogen release. Both scripts are included in Appendix A. The block diagram in Figure 4.8 and Figure 4.9 detail the code process for each.

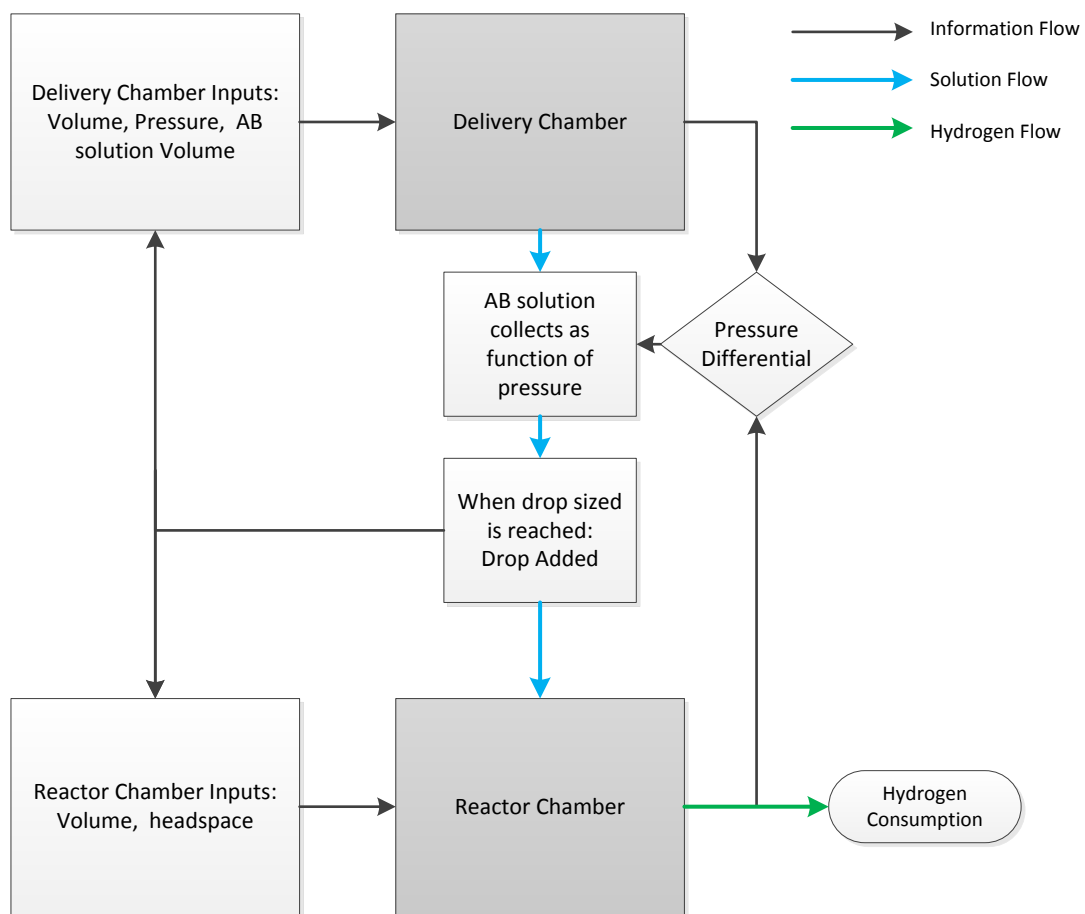


Figure 4.8. Single pressurization: MATLAB flow diagram.

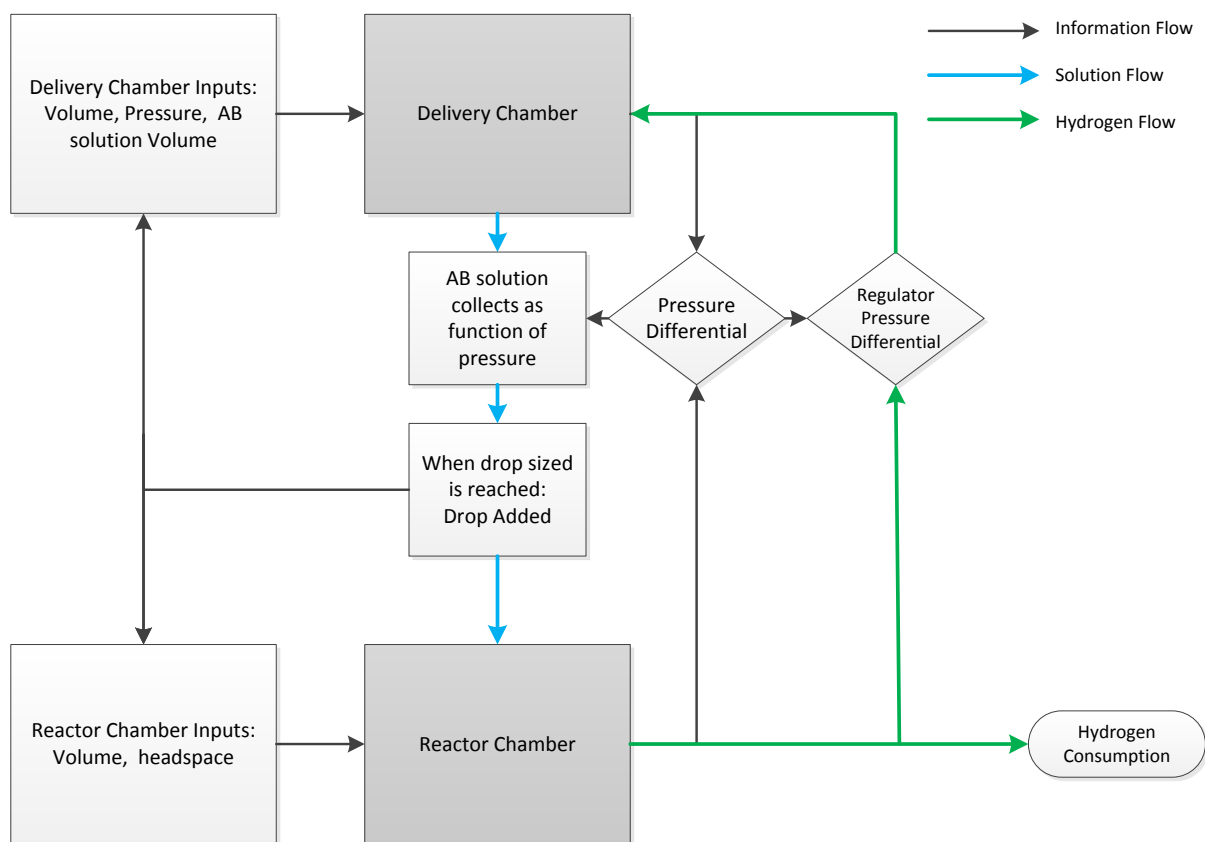


Figure 4.9. Regulated pressurization: MATLAB flow diagram.

When these codes were compared to experimental data, the range of pressure values were accurate, but the exact frequency and period of pressure oscillations given from the code were not precisely aligned. Inconsistent behavior is primarily due to the fact that reaction rate was not fully accounted for in these scripts. An evenly spaced time delay was applied, but was not fully accurate. In order to understand the behavior of both systems, droplet size and rate was determined to predict the effective hydrogen output. Since solution will only flow at the minimum pressure differential, the orifice does not provide stream flow. Rather, drops slowly collect on the orifice face, expanding until they reach a critical size. The average drop size was measured to be 55 μL .

5. RESULTS AND DISCUSSION

5.1 Liquid Mixing Designs

The experimental analysis of designs A and B described in section 3.1.1 are presented here. Design A was tested and a prototype system was verified. A sensitivity analysis was performed to find the limits for the reactor. Design B was also experimentally verified. A comparison between the performances of these two designs was made using experimental data and modeling.

5.1.1 Single Fill

Successful hydrogen flow was achieved for any test in which the pressure inside the main reactor chamber was held above ambient. The pressure of the cuff effectively set the operating pressure of the entire system. Various orifices and cracking pressure check valves were used to adjust the pressure differential between the two chambers. Figure 5.1 shows the typical pressure performance of an air pressurized delivery system.

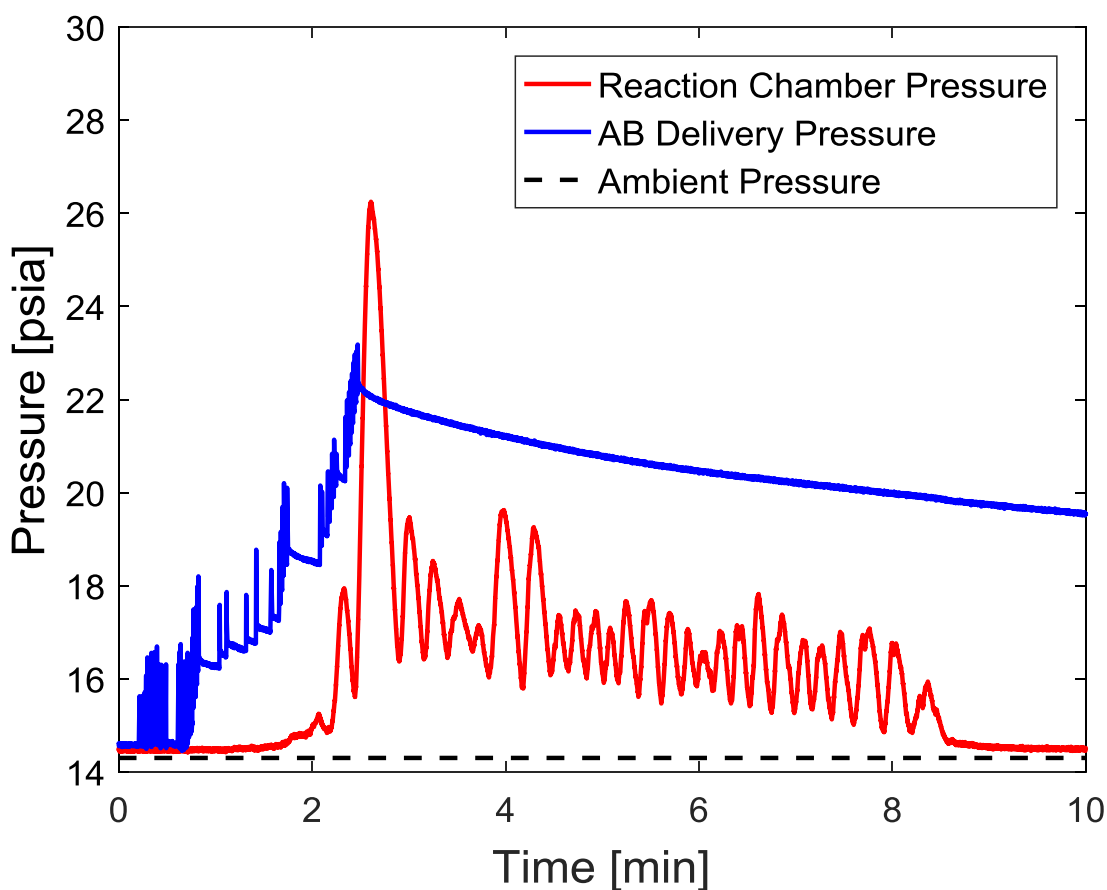


Figure 5.1. Hydrogen pressure performance for pressurized delivery of AB.

The sinusoidal behavior of the reactor is expected to continue until all AB has been delivered or the AB delivery pressure is too low. Sizing of the upper chamber, or the IV cuff, are based on the ideal gas assumption that the pressure will drop proportionally to the volume increase that occurs when the ammonia borane solution is delivered. The initial pressure and volume of the cuff will dictate the duration of a reaction that can take place before a user would have to re-fill the cuff. The minimum allowable pressure is expected at the end of AB delivery and is simply the delivery check valve cracking pressure. As long as the pressure cuff is above this value, the final drops of AB will be delivered. The table below steps through the process of sizing a reactor.

Table 7. Reactor Sizing process.

	Sizing Inputs	Design Feature
1	Select desired mass of AB per charge	M_{AB}, M_{acid}
2	Select on design water addition limited by heat of reaction	V_{AB}, V_{acid}
3	Select delivery chamber max pressure	P_I
4	Select nominal operating pressure of reactor	P_c
5	Size delivery check valve cracking pressure	$P_{cv} = P_I - P_c$
6	Size delivery chamber to remain pressurized for entire charge (V_I)	$P_2 = P_{amb} + P_{cv}$ $P_I * (V_I - V_{AB}) = P_2 * V_I$
7	Size Reactor chamber (V_2)	$V_{hs} = \text{end reactor headspace}$ $V_2 = V_{hs} + V_{acid} + V_{AB}$

The 500 ml pressure cuff was used for all tests, so V_I was oversized for all reactions. In order for there to still be a positive pressure then the volume displacement could be as much as 170 ml of AB solution without any subsequent pressurizations.

After successful testing with the polycarbonate reaction vessel, an identical 500 ml cuff was used to replace the reactor vessel. Housing the reaction in a bag not only increased the gravimetric energy density, but also the volumetric energy density under storage, a key feature for a portable system. Figure 5.2 displays the equipment setup using two IV bags to deliver solution and house the reaction.

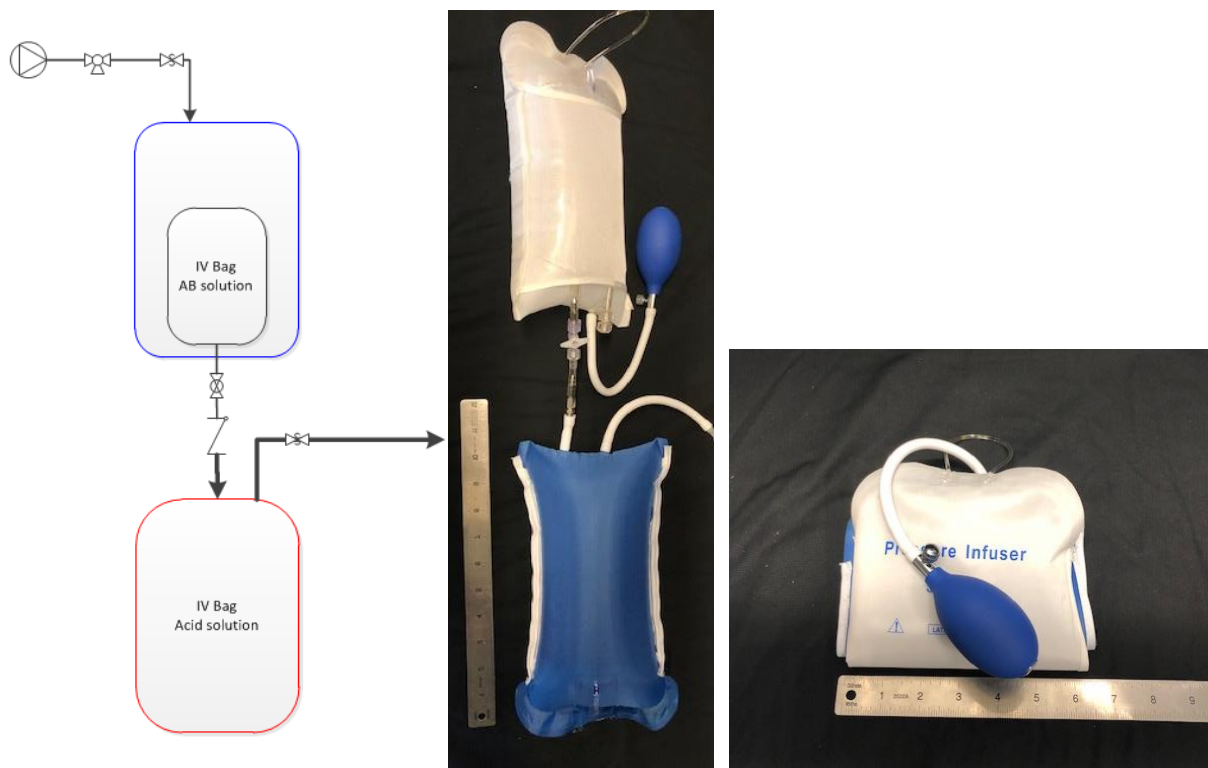


Figure 5.2. Prototype IV bag reactor.

In operation, the system has a volume of 1 L, but under storage can be packed into 4 by 6 by 1 inch (0.4 L). The system's dry weight is 139 grams. The pressure cuff used was determined to have a burst pressure of 41 psia. With the expected maximum pressure in lab conditions being no greater than 27 psia, the system has a factor of safety of 1.52. In the field, the maximum pressure could likely be higher, a topic to be discussed below. To mitigate the risk of bursting, a relief valve should be placed in line of the hydrogen flow line. Reaction bags with higher pressure ratings would also likely be designed for a fielded system. Fuel safe bladders used for vehicles, for example, use ballistic nylon sleeves to hold the PVC liner.

The bag reactor was tested at various conditions to prove repeatable performance. Figure 5.3 demonstrates a test performed utilizing 3 grams of AB being delivered to match four different flow rate values.

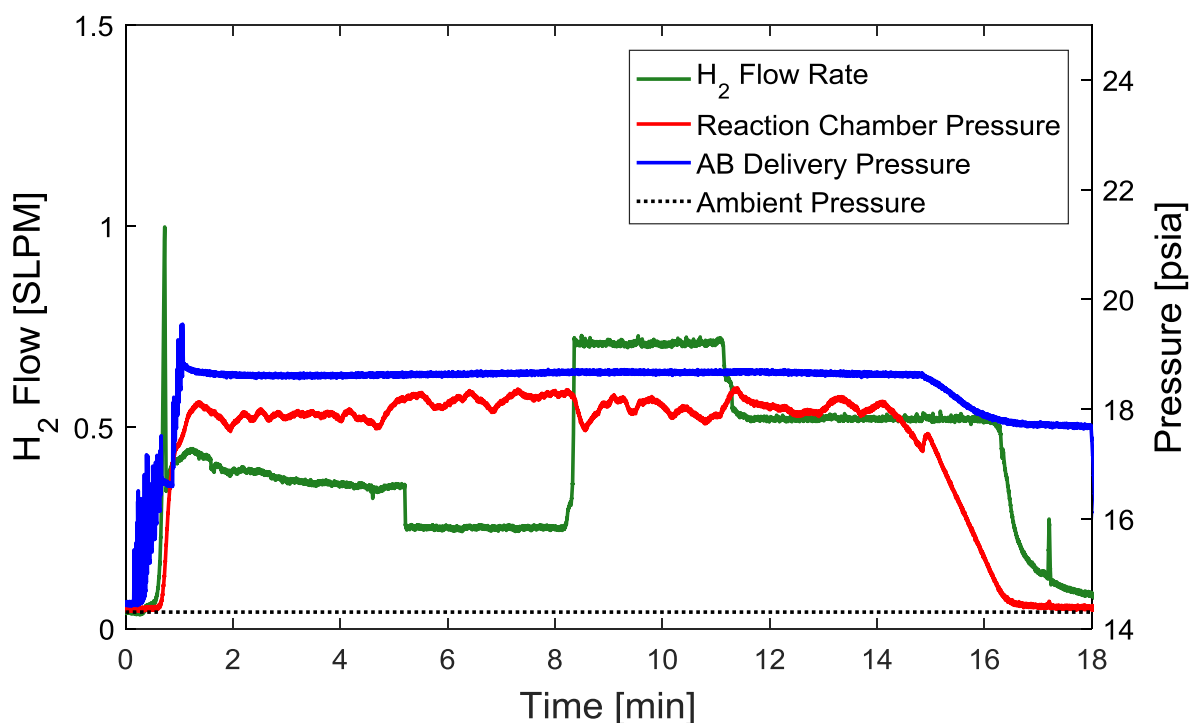


Figure 5.3. Performance of IV reactor at various H₂ flow rates.

The reactor was able to adjust the rate of hydrolysis to match four individual flowrate requirements. An adjusting hydrogen consumption is used to represent the real world conditions expected from a fuel cell with varying loads. The lower load is used to represent a power draw of near 15 W while the upper flow rate would expect to power up to 50 W. Throughout the 16 minutes of operation, the reaction chamber pressure experienced slight adjustments to accommodate the flow change, but remained within a one psi range regardless of the consumption.

Sensitivity Analysis

In addition to the changing load requirements, a field ready system must be able to operate under strained environmental conditions and must be resilient to off design inputs. Three of the assessed performance metrics are reactor pressure, solution temperature and hydrogen purity. A sensitivity analysis was performed using the prototype bag system described above. All metrics were assessed using the following system parameters. In order to match the size of the reactor, the system parameters were set by selecting 10 grams of AB for a single charge.

Table 8. Prototype design values.

System Size		On-Design Factors	
AB mass [g]	10	Water added to AB [ml]	60
Acid mass [g]	37.6	AB concentration [g/ml]	0.1667
IV bag [ml]	300	Water added to Acid [ml]	376
Delivery cuff [ml]	500	Acid concentration [g/ml]	0.1
Reaction bag [ml]	500	Tilt	0°
Cuff Pressure [psia]	22.4	Temperature [°C]	23
Pressure drop [pisa]	2.33	H2 flow rate [sLpm]	0.52
Orifice [inch]	0.020	Maximum expected	50
Vent Pressure [psia]	40	solution Temperature [°C]	

Figure 5.4 shows the sensitivity of reactor pressure to agitation, orientation and water addition. Water addition values are presented in a fill percent of the total volume of each vessel. The maximum fill for the reactor vessel is 88%, or 440 ml because after all 60 ml of AB is added, there will be no available headspace. The same reasoning sets the maximum fill for the AB solution to 41% (124 ml). The lower fill percent limits (5 and 10%) are set by the volume of the reactants as if there were no water added. Red bars indicate the bounds of ideal operating conditions, as pressure is above ambient and below the vent pressure. Each box on Figure 5.4 represents the expected pressure range that a given parameter will induce when it is adjusted.

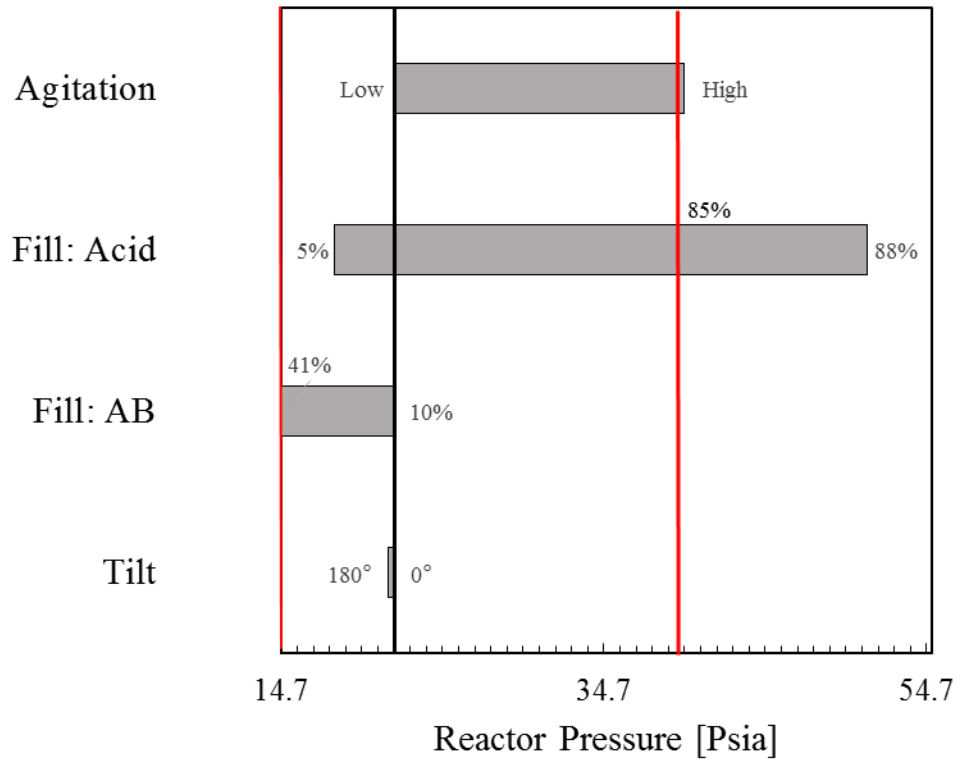


Figure 5.4. Sensitivity analysis based on MATLAB modeling.

With the possibility of use under movement, a system must be resilient to agitation and constant movement. An event of mechanical agitation will cause a momentary spike in pressure due to the increased mixing of the reactants. Once a steady rate of shaking is achieved, the reactor should settle into nominal pressure performance similar to the response of dropping the hydrogen consumption rate. The worst case scenario is that a single event of shaking causes the pressure to spike above the reactor relief pressure.

Operation orientation is another consideration. Table 1 shows that some military grade fuel cell systems are limited in their operating orientation. The two factors effected by orientation for a liquid delivery system are solution flow and hydrogen flow. Gravity will either work with, or against the pressure gradient to deliver the AB. For the IV delivered AB, a 180° tilt angle (upside down orientation) will still deliver solution, but drop the nominal reactor pressure since the effective check valve pressure has increased. With a solution transfer distance of 5 inches, upside down orientation will increase the cracking pressure by approximately 0.35 psia. In regards to hydrogen flow, the system depicted above is not currently capable of flowing hydrogen at any

orientation where solution is exposed to the hydrogen flow line. Further design work would need to occur for the hydrogen flow line to remain uncovered by liquid.

The system must also be insensitive to the water that is available to a soldier. Water sources may be limited in both quality and quantity. Additionally, human error must not lead to catastrophic failure in the case of overshooting the on-design fill levels. Using the MATLAB model, expected pressure performance was predicted for a range of water fill levels. Looking first at the AB solution, filling the IV bag to its full 300 ml will both dilute the solution and cause the pressure cuff to deflate faster. As mentioned earlier, the lowest volume of water to dissolve the 10 grams of AB is 26 ml. The highly concentrated solution will cause a slightly higher spike in pressure for each drop, but will not cause a significant rise in nominal pressure as long as all other parameters are at the design value. For the reaction chamber, the lower limit is completely dependent on temperature. Even with the largest possible headspace (500 ml), there will still be a positive pressure of hydrogen. On the other hand, adding too much water to the reactor will cause issues with headspace limitations. The primary concern is the reactor completely filling with the addition of AB and either venting out solution or driving solution through the hydrogen flow line to the fuel cell. Both situations will result in a pressurized reactor that could be difficult to empty. Any fill amount greater than 85% (425 ml) will result in a pressurization above 40 psia by the end of the reaction due to the limited headspace. The upper limit for reactor fill level is set at 85%.

The lower performance bound for the reactor fill was determined using an adiabatic solution temperature analysis of equation 4 displayed in Figure 5.5.

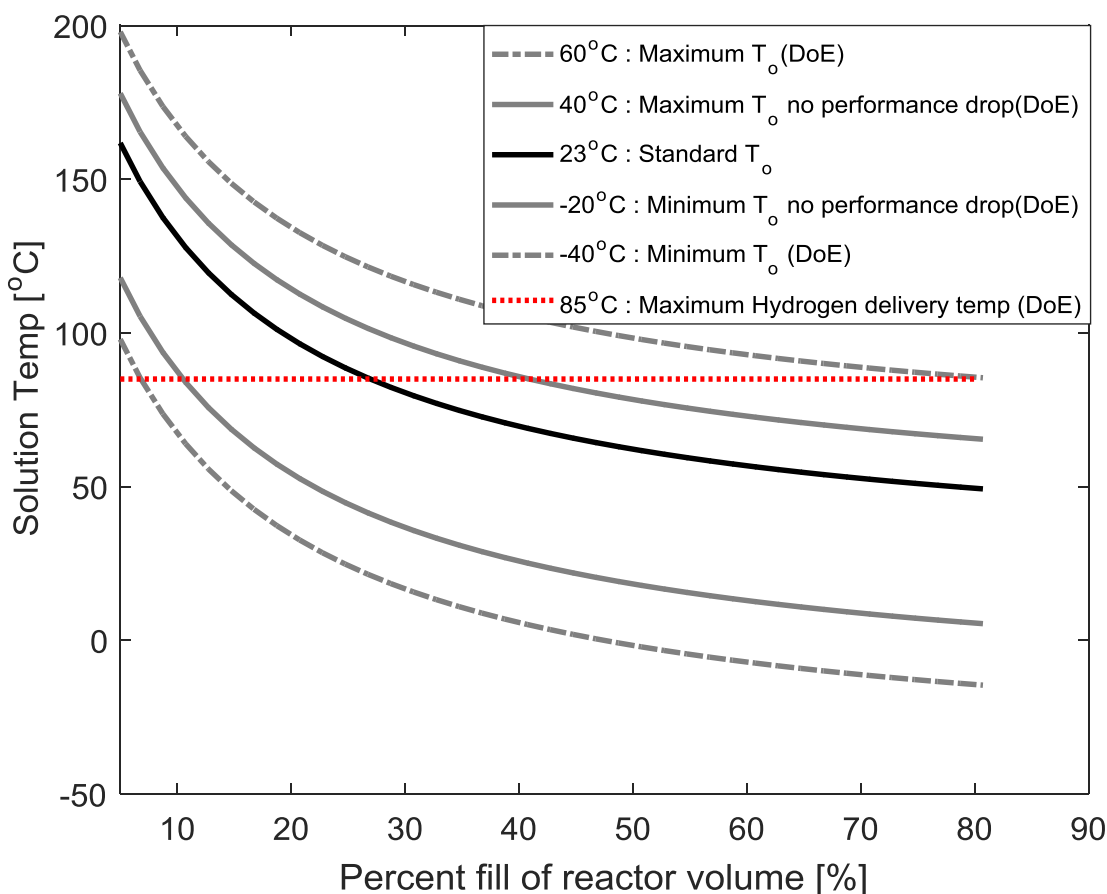


Figure 5.5. Theoretical maximum reaction temperatures.

The temperature analysis assumes adiabatic conditions and constant specific heat values since there is a relatively low temperature range. Maleic acid was not accounted for in the heat of formations, but was considered for the total specific heat value. Final temperature at the end of reaction will realistically be lower than the presented values since heat transfer through the reactor walls and convective cooling on the outer surface was not taken into account. The adiabatic assumption is more realistic at lower volumes since there is minimal contact with the reactor wall. The expected temperature was plotted against reactor fill level at five ambient temperatures. The absolute upper and lower temperature limits (60 to -40°C) were taken from the DoE standard for portable devices. The same standards set -20 to 40°C as the range where performance degradation is not allowed. These tighter bounds were used for designing a system since they aligned more closely with the limits of the 2590 battery set in MIL-STD 810. The DoE's standard of maximum hydrogen delivery temperature of 85°C was used as the maximum allowable solution

temperature [22]. With these constraints, a 40% fill was selected as the lowest allowable fill volume. If sufficient water is not available to fill to 40% of the reactor volume, the total amount of AB should not be delivered to the reactor.

Water quality is an important consideration as well. In the case of particulates and impurities, AB solution flow could be hindered by clogging. A water source with potentially catalytic properties also pose a problem for the AB solution. For these two reasons, high quality water should be prioritized for use with the AB. Previous work on this project demonstrated effectively pure hydrogen release for a range of water sources including seawater, urine, soda and rainwater. Additionally, a slightly acidic solvent will aid in the promoted hydrolysis of AB.

5.1.2 Regulated Fill

The regulated hydrogen fill design is fundamentally more sensitive to the volume sizing for both vessels. Unlike model A, a re-filling design requires the reactor chamber pressure to exceed the upper chamber pressure for hydrogen to be delivered. Testing design B proved difficult if careful attention was not given to the sizing of each component, resulting in behavior shown on the left of Figure 5.6.

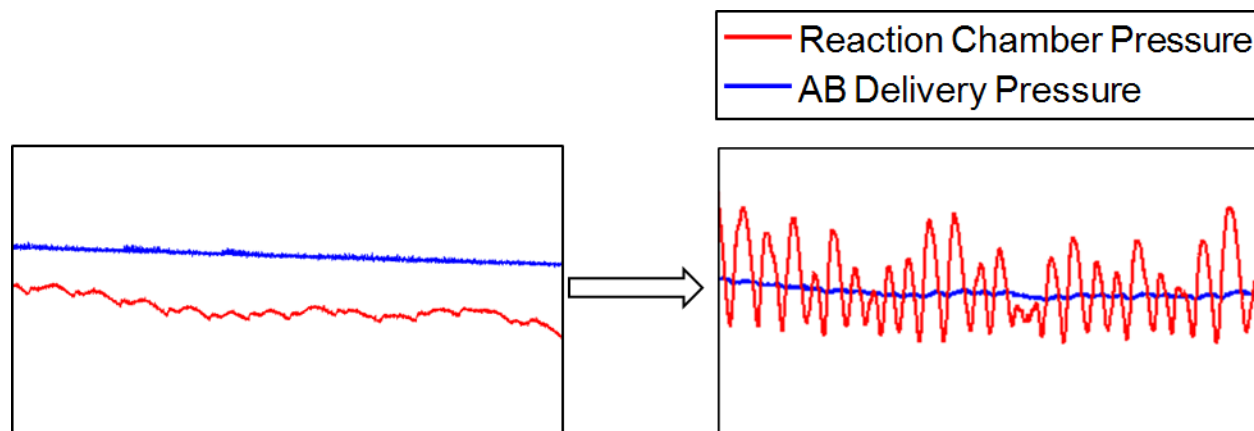


Figure 5.6. Ideal pressure behavior for regulated fill system.

To design for the pressure trace on the right, the average operating pressure in the reactor must be brought closer to the delivery pressure. This can be achieved by decreasing the effective cracking pressure between the cylinders. Larger orifices and shorter lengths of tube were needed for this system. Reactor pressure cannot be steady, as this system depends on high amplitude oscillations around the design operating pressure. The amplitude of these pressure spikes is greatly

affected by the concentration of the AB, the hydrogen consumption rate and reactor headspace. Figure 5.7 shows the performance of a successful test that allowed the reaction chamber to produce enough pressure to fill the delivery vessel with hydrogen.

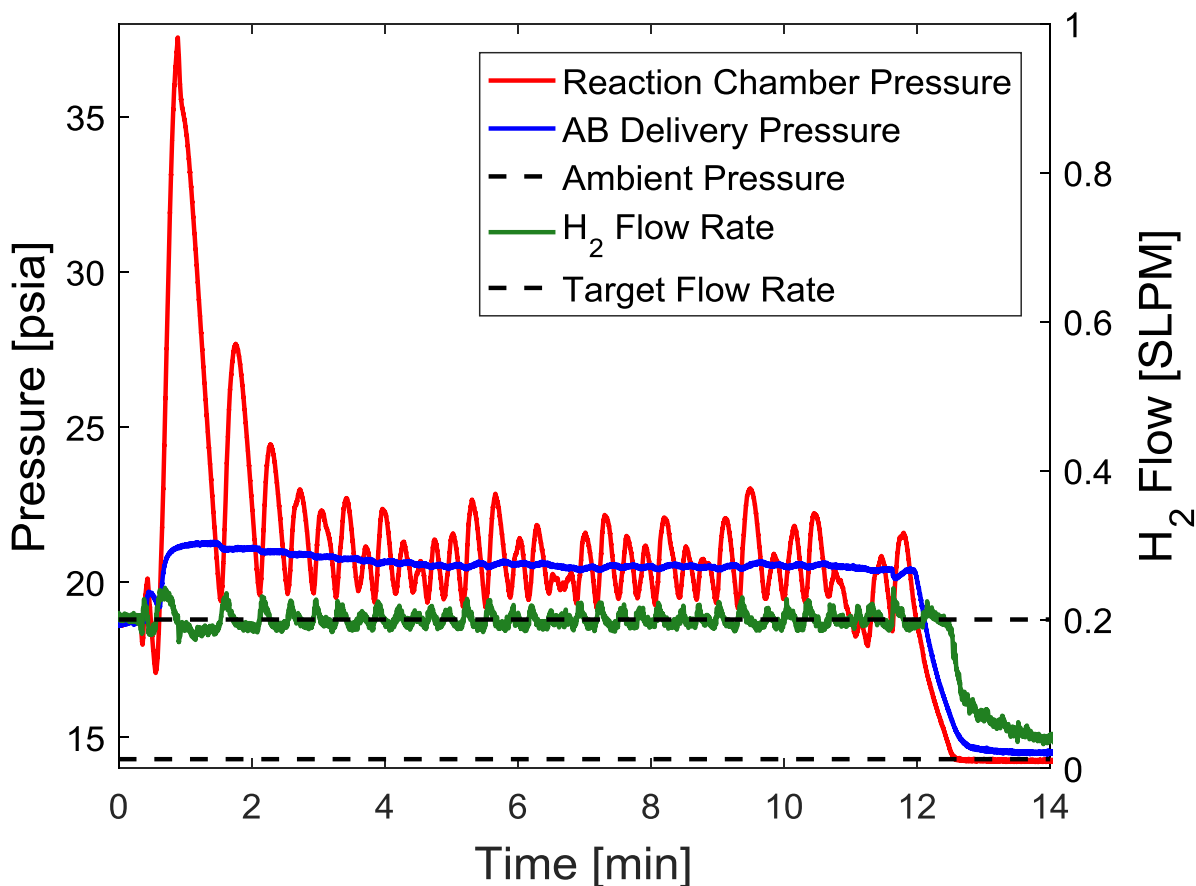


Figure 5.7. Hydrogen pressure performance for regulated pressurized delivery of AB.

Figure 5.8 focuses into a region of the previous pressure trend and describes the factors that influence the shape of the pressure curve. The check valve cracking pressure is the pressure that the chamber pressure would settle in at in an immediately responsive system. Drastic oscillations are due to the slow response time of each drop's correlated hydrogen flow.

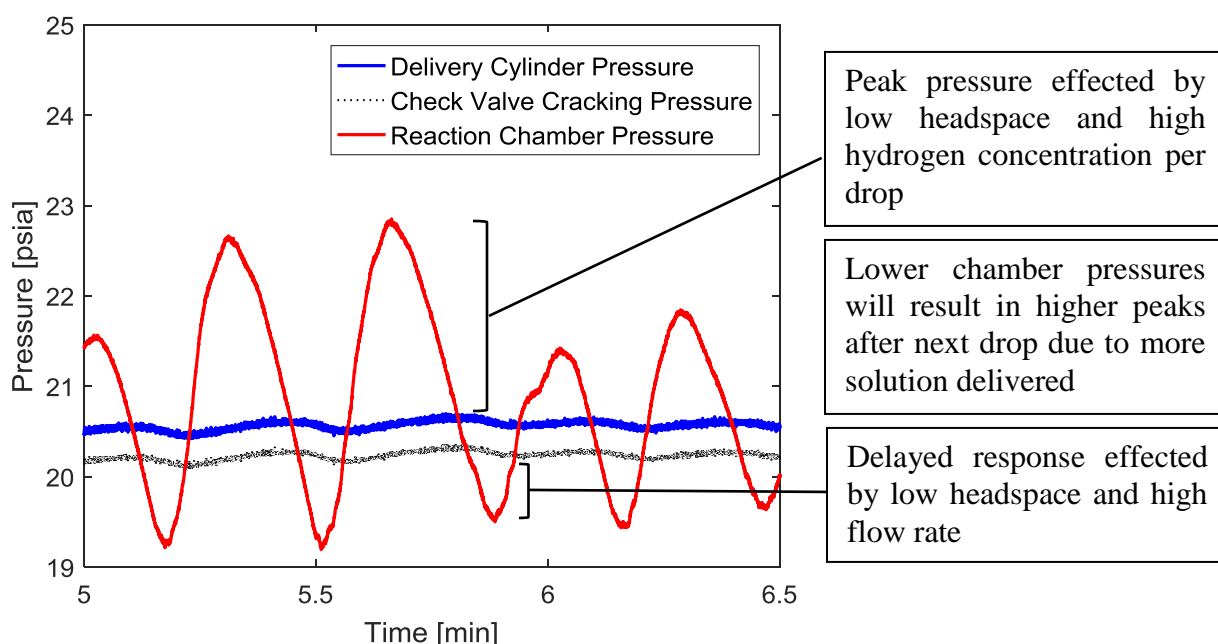


Figure 5.8. Explanation of regulated fill pressure.

Returning again to the 10 grams AB design profile, the advantage for this architecture becomes the reduction in delivery headspace. At the same conditions described in table 8, this system will allow for the upper chamber, labeled delivery cuff, to be reduced in volume from 500 ml to 90 ml. While the overall weight savings are negligible due to the added mass of the regulator, the primary benefit is in volume reduction.

For a system of this size, a sensitivity analysis for this design would yield similar limitations as discussed above. The primary difference is that this reactor is now constrained by the lower limit of water added to the reactor. For a given hydrogen consumption rate, there is a maximum headspace that will collect enough pressure for hydrogen to flow to the upper chamber. If this critical headspace is not reached, then the reaction will stop until more AB is manually pushed into the reactor by an external pressurization. The headspace is dependent on both the size and concentration of the AB drops as well as the hydrogen flow rate. At the AB concentration of 0.1667 g/ml, an average drop size of 0.55 μL and flow rate of 0.52 sLpm, this headspace is theoretically around 140 ml based on the MATLAB code. Experimentally, at these conditions, hydrogen failed to fill the delivery chamber when the headspace dropped from 180 to 170 ml. The same test however instantly re-pressurized when the headspace started at 60 ml. To confirm the

theoretical critical headspace, a test should be conducted with a starting headspace above 140 ml and a finishing below. With around 100 ml of working headspace, this system will perform like Figure 5.7 for small scale designs. Scaling this system up would require more available headspace. Larger pressure oscillations could be attained by increasing the AB addition rate, however this will negatively affect the systems performance at low headspace. In order to ideally size a scaled up system, the delivery chamber can be pre-pressurized so that AB can be initially delivered while the headspace is above the critical value. Figure 5.9 shows the predicted performance of a system that is initially pressurized to its regulated pressure. Figure 5.9 is a result of the MATLAB code with the inputs from Table 9.

Table 9. 20 gram AB reactor design.

System Size		Inputs	
AB mass [g]	20	Water added to AB [ml]	120
Acid mass [g]	75.2	AB concentration [g/ml]	0.1667
Delivery vessel [ml]	320	Water added to Acid [ml]	752
Reaction vessel [ml]	920	Acid concentration [g/ml]	0.1
Delivery Pressure [psia]	22.4	Tilt	0°
Pressure drop [pisa]	2.33	Temperature [°C]	23
Orifice [inch]	0.020	H2 flow rate [sLpm]	0.52
Vent Pressure [psia]	40	Maximum expected solution Temperature [°C]	50

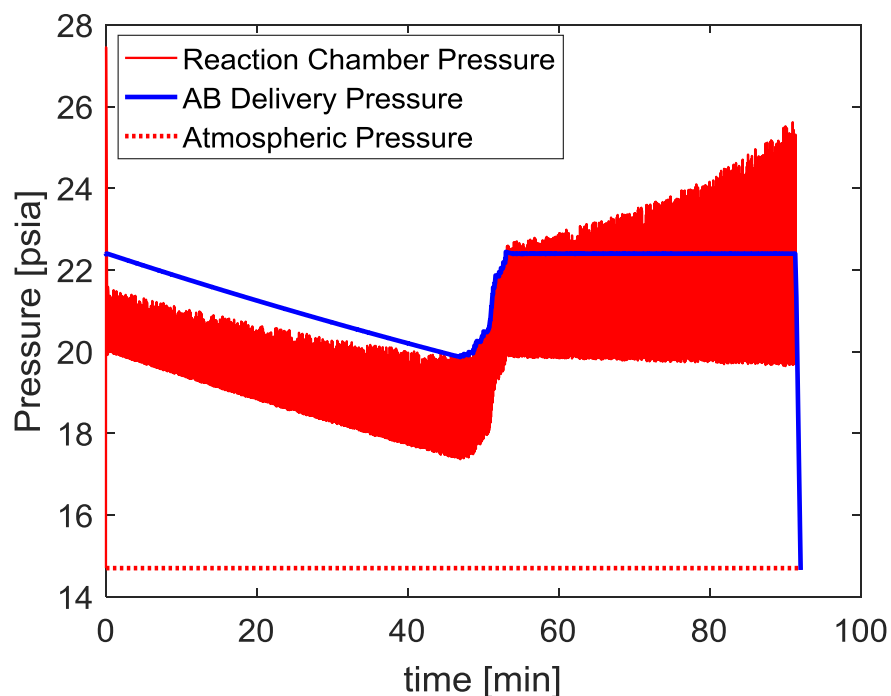


Figure 5.9. Model of ideally designed 20 gram AB system using hydrogen pressure.

Over fifty percent of the test will behave like the single pressurization system. As AB solution is delivered into the reactor, the headspace in the reactor will grow smaller. Once the critical headspace is reached, the chamber pressure will rise enough above the delivery pressure to begin filling the upper vessel. From this point onward, the system will behave as described in Figure 5.8. Using an identically sized system, the same MATLAB analysis was performed for model A shown in Figure 5.10 a).

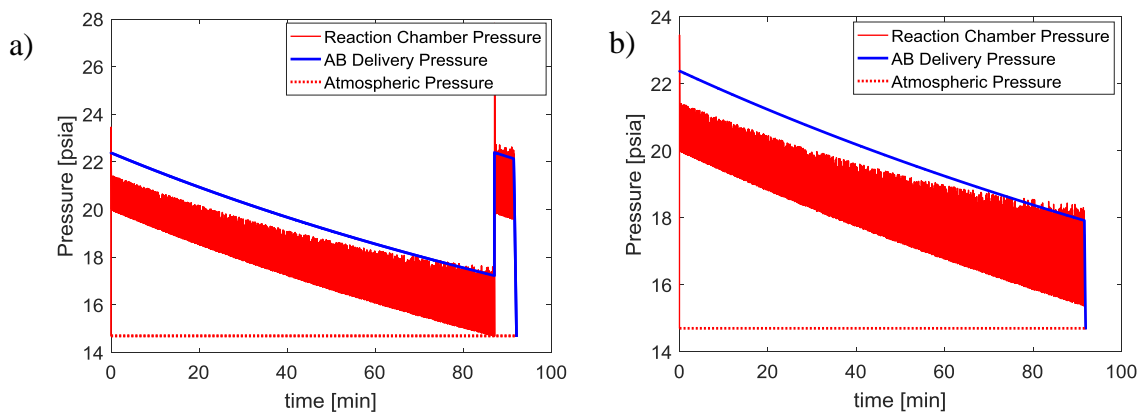


Figure 5.10. a) under sized b) ideally sized, 10 gram AB system using single pressurization

Figure 5.10 a) shows that the troughs of the pressure oscillations will dip to ambient pressure, requiring the cuff to be re pumped with air for all AB to be delivered. The increase in pressure at 90 min represents the user manually filling the cuff to the desired pressure. In Figure 5.10 b), the initial headspace of the reaction chamber is increased by 70 ml by reducing the amount of water added to the acid. Such changes are enough to extend the system to full delivery. Alternatively, the cuff pressure could have been increased to 23.6 psia, the delivery volume by 100 ml or a partial combination of the two. The primary advantage that the single pressurization performance reveals is that the driving pressure is very low at the end of the reaction. This is a safety feature if too much water is added, as the pressure will flat line at a relatively lower pressure. The regulated system will continue to push AB into a pressurized vessel due to the high hydrogen pressure expected at the end of the reaction. A runaway reaction will ensue until hydrogen stops flowing out. Additionally, having the lower fill limit dependent on temperature rather than a critical headspace is advantageous because cooling methods can be used in the future to reduce the water requirements.

While this system can theoretically sustain a longer duration charge for the same component sizes, its complexity and sensitivity reduce its value greatly. The system design was ruled impractical for a man worn system due to the added weight of the regulating components, the sensitivity to the amount of water added and its minimal improvement in performance. Additionally, two pressurized chambers of hydrogen is less desirable than one. One of the main issues that would have to be addressed to make this system feasible, is separating the air in the delivery vessel headspace from hydrogen.

5.2 Solid AB

The experimental analysis of solid AB hydrolysis described in section 3.1.2 is presented here. The single chamber design provides the simplest architecture for a controlled reactor. A single reactor design will have the same temperature constraints associated with lower fill levels of water. Depending on the design, the risk of over pressurization due to adding too much water could be subsided. These designs will also be insensitive to potential freezing and poor water quality. The first step in designing a practical solid AB reactor is understanding the interaction between solid packed AB and an acidic solution.

Ammonia borane pellets encased in epoxy proved to be chemically and physically stable. Testing with these sample pellets provided repeatable hydrogen release trends shown in the figure below. It was confirmed through experimentation that having the AB surface upwards facing provided the most consistent flow results since bubbling did not interfere with surface area contact. Four upright pellets ranging from 0.55 to 0.75 grams of AB were tested in the same molar concentration of maleic acid solution. The hydrogen flow result are shown in Figure 5.11.

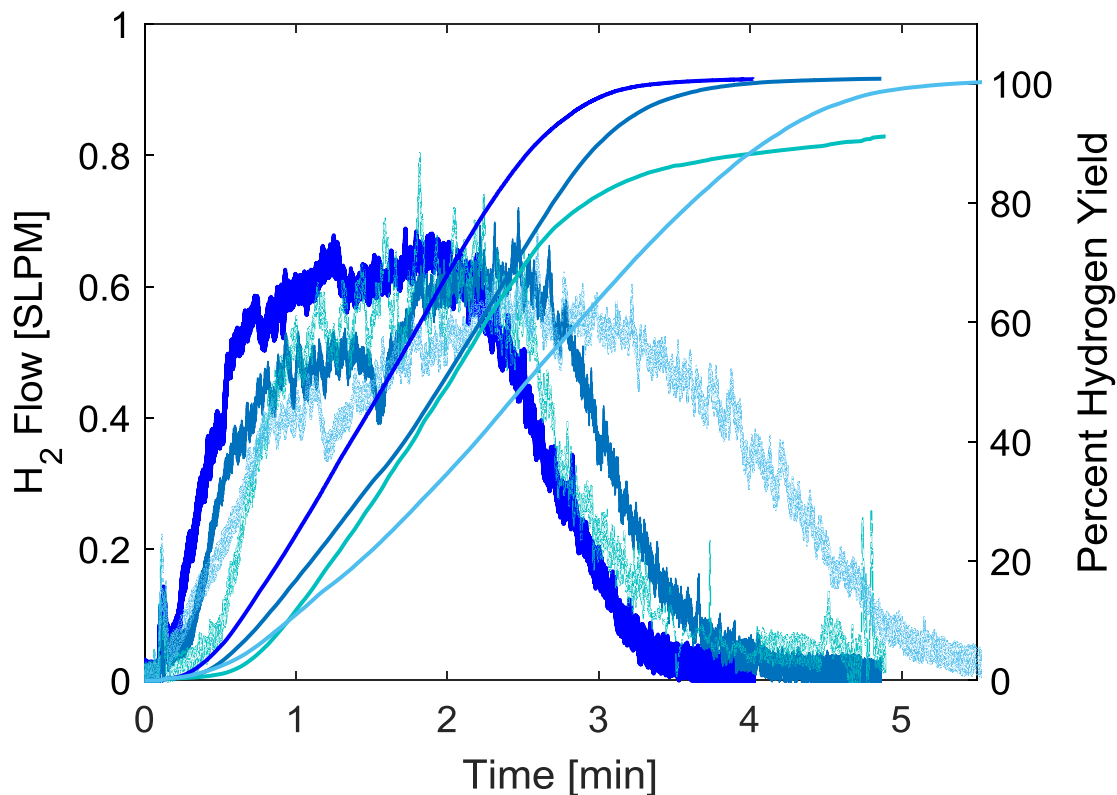


Figure 5.11. Repeatable H_2 flow from $\frac{1}{2}$ inch diameter AB pellets.

Theoretically, an even regression due to hydrolysis would yield a flow rate that plateaus at the rate associated with the exposed surface area. While a steady state flow is not fully achieved for any of these tests, the flow appears to settle around 0.6 sLpm for each pellet, with an average peak flowrate of 0.696 sLpm. Neglecting surface porosity, the exposed area of AB in the $\frac{1}{2}$ inch diameter pressed pellet was 0.19 in^2 . This would equate to a flow rate per unit area of $3.53 \text{ sLpm}_{(H_2)} / \text{in}^2_{(AB)}$. In an effort to identify if the flow from these pellets will reach a steady state or continue to increase, longer pellets were pressed containing 2 grams of AB. Figure 5.12

shows the flow performance of two pellets made from the same AB batch and reacted in the same concentration of 1 equivalence of maleic acid. The first pellet, shown in green, contained 0.55 grams of AB and was 0.22 inches high. The second pellet, shown in grey contained 2.1 grams AB and was 0.88 inches high.

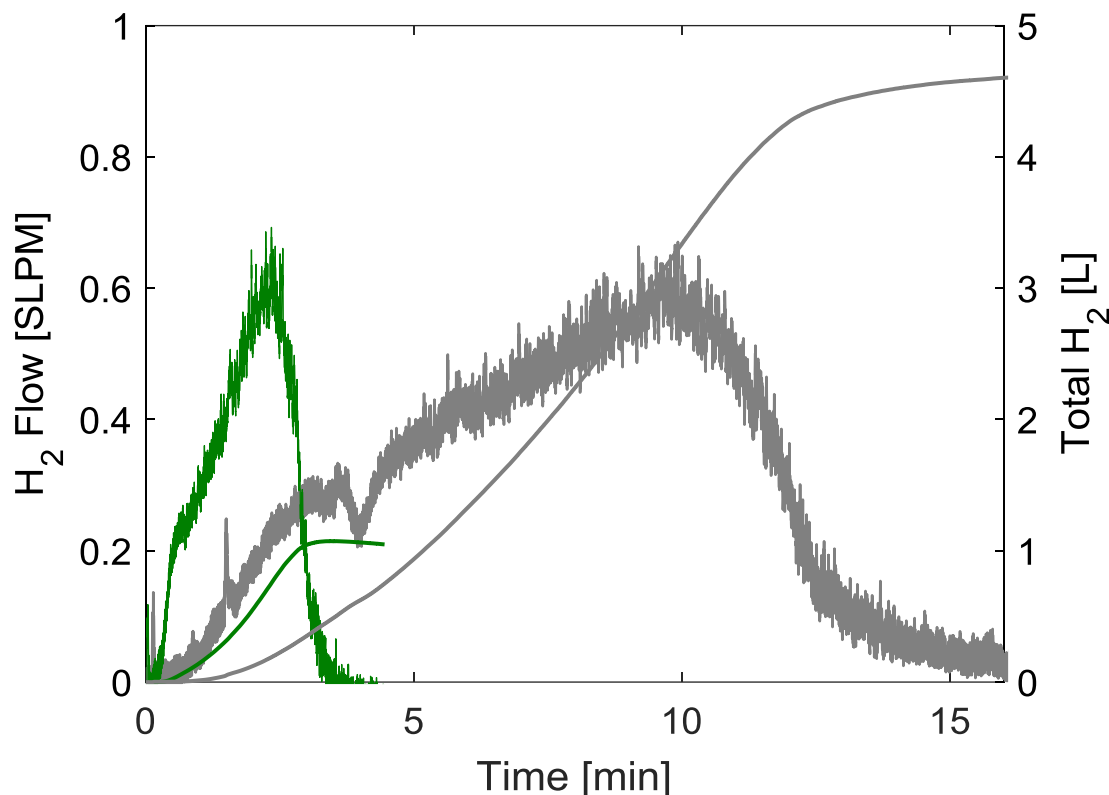


Figure 5.12. AB pellets with differing lengths and solution height above surface.

Between these two tests, the only changing variable was column height above the AB surface. The amount of water and acid added for the series of tests was proportional to the mass of AB, and since the reactor had a constant diameter (2 inch), the headspace did not scale proportionally. The shorter pellet had an initial column height of 0.49 inches while the longer pellet had 0.3 inches. Considering all other equal parameters, it is hypothesized that the circulating headspace of acid available to contact AB effected the rate of hydrolysis. Additionally, the added column height will provide a greater hydrostatic pressure at the reaction interface. The increase in force could be enough to promote reaction kinetics on a slightly porous surface. For these tests, longer pellets

never achieved a superior flow rate because they reacted much slower. Further work should be done to confirm the trend and test the hypothesis.

In order to account for the reduced headspace, an additional test was performed with 2 grams of AB and an initial column height of 2 inches. Excess acid and water was used to keep the solution at the same concentration. Figure 5.13 shows the hydrogen release of this pellet in red.

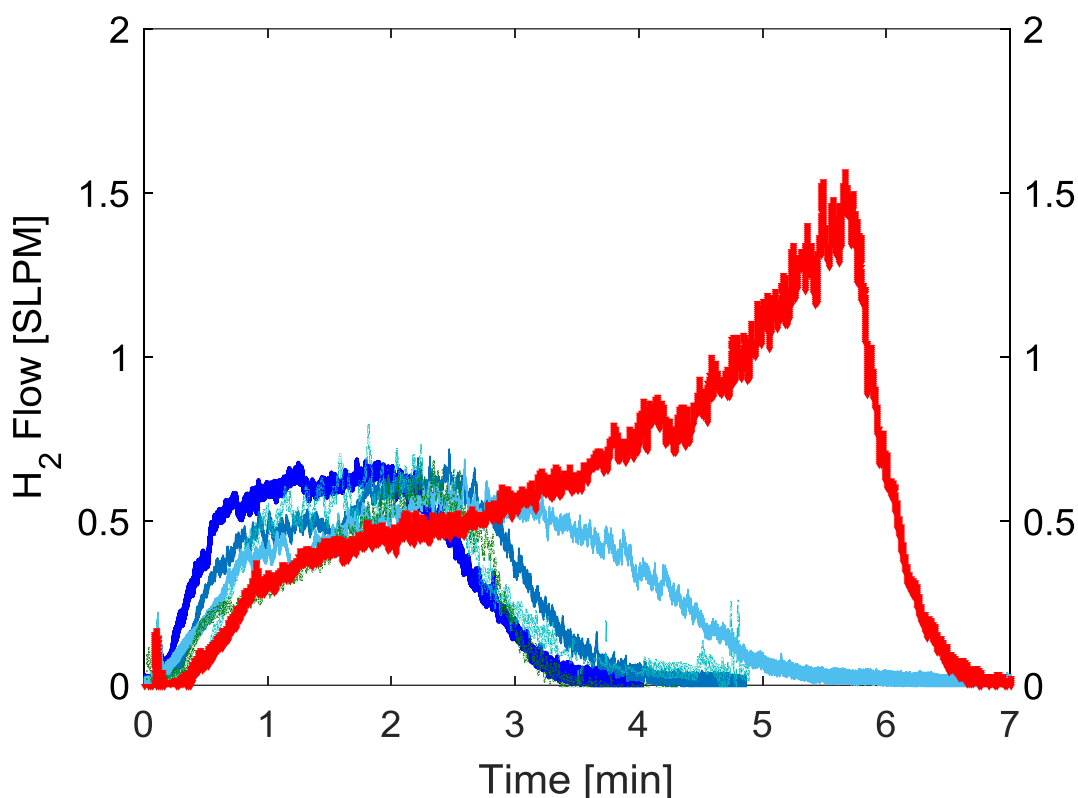


Figure 5.13. Extended duration test with excess solution height.

The initial two minutes look comparable to the initially repeatable behavior shown in Figure 5.11. The hydrogen released at 2.5 min is 0.8 L, associated with approximately 0.33 grams of AB. The tests depicted in blue were all within 0.55 to 0.7 g. Instead of plateauing, the hydrolysis rate continues to increase exponentially. It cannot be assumed that the hydrolysis rates for all pellets would continue to increase if they were larger since this test was not thoroughly repeated. The behavior could have been an anomaly in which the pellet was dislodged from the epoxy casing and caused an expedited reaction. Despite the variation for each test, a general trend was noticed of a steady increase in the amount of hydrogen being produced.

Part of this increasing trend is due to the fact that all of the AB does not appear to instantly hydrolyze with the acidic solution; instead, some fraction is either suspended or dissolved in solution. Immediately upon submersion into the acid, the AB surface begins to emit hydrogen bubbles. Within seconds, bubbles begin to form throughout the reaction vessel as shown in Figure 5.14. Visually recording the reaction is hindered from excessive bubbling on the cylinder walls by two minutes into the test.

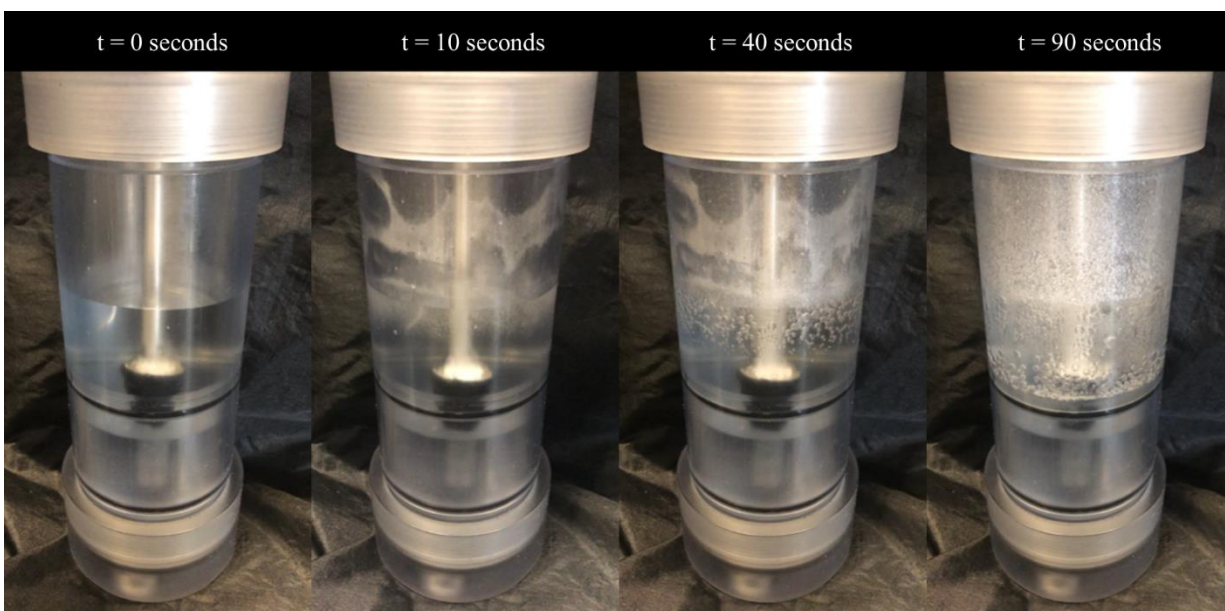


Figure 5.14. Progression of AB pellet testing.

Even after the pellet was fully dispensed of all solid AB, the reactor continued to off gas hydrogen as AB in solution continued to react. It was unclear whether this AB dissolved on contact with the solution, or particles were dispersed off of the surface due to the kinetic action of bubbling. If particles were discharged, pitting would likely occur on the surface making the AB more porous as the reaction continues. In addition to this, reaction temperature is constantly rising, causing dissolvent and kinetic rates to increase.

In order to investigate surface morphology, SEM images (shown in Figure 5.15) were taken to compare a pellet sample before and after it was submerged in maleic acid solution. The surface to the left of the dotted line is the pellet's surface area in greyscale after it was pressed. The right shows the same surface location after it was submerged under 2 inches of maleic acid solution and allowed to bubble.

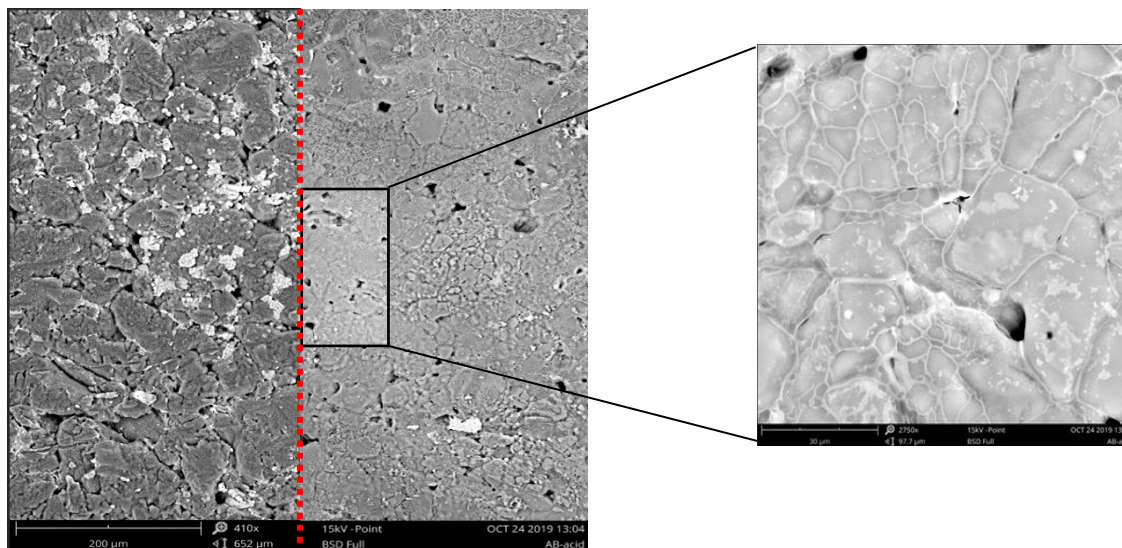


Figure 5.15. 410x SEM imaging of AB pellet before (left) and after (right) acid exposure.

3-D surface roughness mapping indicated that the Rz values for this surface went from 1005 nm to 1540 nm after acid addition. Ra values were on the order of micrometer and were considered unreliable. Further investigation is required to assess the surface behavior and confirm if pitting is occurring.

Another possible causation for the rise in hydrogen flow shown in Figure 5.13 (red curve) was that channeling could have occurred on the interface between the AB and the epoxy. If this were the case, this would explain the progressive rate at the beginning due to the increasing surface area contact as the edge contact increase. Once the solution has penetrated the edges all the way, the surface area will begin to decrease. From visual inspection, this did not appear to be the case as the AB dissolved evenly when pellets were removed mid reaction.

5.2.1 Applications

Hydrolysis from solid ammonia borane provides many advantages. One issue that has been arising during the work of this thesis was the stability of ammonia borane in solution. Even with pure AB and de-ionized lab water, un-catalyzed gas release has occurred through experimentation. Additionally analysis would identify these gasses as ammonia or hydrogen. Ammonia air bubbles in the ammonia borane solution pose a great risk for the PEM fuel cell. Designs with the intent of separating these bubbles in the acidic solution have not been successful. Hydrolysis occurring at

the surface area of solid AB and acidic solution mitigates these issues since the initial reaction is in an acidic environment. From a user point of view, the simplicity of only mixing one solution is desirable. The risk of human error is mediated, as there will be no chance of switching reactants and carrying and maintaining one reactor leaves less room for system damage. Eliminating the AB delivery chamber and any mechanisms associated with AB delivery also improves the systems energy density. The energy density with respect to storage can also benefit from the fact that storage components of solid AB could serve a dual purpose of controlling hydrolysis. The epoxy coated pellets for example are sealed and contained by the same shell that helps maintain reaction rate. Likewise, a cordierite monolith both holds AB and controls the rate of solution flow. As mentioned earlier, the main issue with either the controlled release pellet or catalyst bed reactor design is that a constant release of hydrogen is not sufficient for a fuel cell with varying loads. Any system utilizing solid ammonia borane needs further work in designing a pressure regulated control mechanism addressed in section 3.2.1. Whichever design is selected, predicting hydrogen release must factor in both direct AB-Acid surface area contact as well as residual AB that is continuing to react in solution. The responsiveness of a pressure dependent reactor will depend on the release characteristics. Another consideration is the stability of AB surfaces after removal from acid solution. A major drawback to solid AB designs is that all of the AB is contained in the reactor for the entire reaction. If violent bubbling induces pitting, then the AB structure could experience structural weakening. If pitting is enhanced as the surface is further roughened and as temperature increases, a larger pellet could experience pitting to the point of cracking or dislodging.

5.3 Revisit Trade Study

Near the end of this research, the trade study discussed in section 3.3 was revisited. Changes were made to the rankings of each system based on the properties that were observed in experimentation. These changes are highlighted in the revised Pugh chart in Table 10.

Table 10. Concluding Pugh chart analysis.

	Increased
	Reduced

				Peristaltic Pump	Single Pressurization	Regulated H2 flow	Controlled Release Pellets	Monolith Catalyst Bed	Pressure dependent exposure
	Property	Weight		A	B	E	F	G	
1	Robustness	3	D	2	-2	0	0	0	0
2	Energy density	3		2	1	1	-3	0	0
3	Safety	3		0	-1	-2	0	-2	0
4	Reactor storage	3	A	1	0	2	2	1	1
5	Reactant storage	2.5	T	0	0	1	-1	1	1
6	Autonomy after initiation	2		0	0	0	0	0	0
7	Refill procedure	2	U	0	-1	2	-1	2	2
8	Set-up procedure	1.5	M	0	-1	3	2	2	2
9	Take down procedure	1.5		0	0	2	2	2	2
10	Orientation for operation	1.5		1	0	3	-1	-2	-2
11	Production/Cost	1		2	1	2	-2	0	0
	Rated as: (-3, -2, -1, 0, 1, 2, 3)	Total	0	18.5	-8.5	23.5	-5	6.5	
		Original	0	11.5	-5.5	27.5	1	12.5	

The single pressurization system improved on the reactor storage due to the compatibility of IV bags and cuffs; components that were not originally assessed. Design A's autonomy was originally thought to be negatively impacted by the assumption that a user would constantly have to re-pump the delivery chamber to feed all the AB solution. However it was found that an optimally sized design for a small scale charge would require only one pump and not require excessive volumes.

For the regulated flow design, its overall robustness (a measure of sensitivity to factors mentioned in Chapter 5) was initially higher than what was proven with system level testing. Complications involving purging air and sensitivity to over pressurization make this system less robust than what was originally predicted. The robustness rankings were also lowered for all solid

AB designs due to their inconsistent behavior with varying acid column height and potential corrosive nature of solid AB. The safety of a pressure dependent system with solid AB was also lowered because of this uncertainty. Housing AB in the main reactor when it could break apart raises the risk of a runaway reaction and potential for an explosion. Overall, the single pressurized delivery architecture outranked the solid AB design. Though this scoring is somewhat subjective and the values are so close, a situational assessment must be performed to account for the advantages and disadvantages of both systems. Given the current priorities of a reactor design, the ideal reactor design is the single pressurized delivery of AB into a reaction chamber.

6. CONCLUSIONS

On demand hydrogen from chemical hydrides such as ammonia borane is a promising alternative energy solution. As the industry of PEM fuel cells continues to grow, chemical hydride systems could be an attractive energy storage method for dismounted military units. Soldiers would use a fuel cell charging device to compliment the electronic systems that they rely on for mission success. My thesis focused on optimizing a combat ready hydrolysis reactor design. The goal was to present an AB delivery mechanism that operated independently of electrical inputs in order to increase the system's durability. An overview of testable parameters and performance validation metrics for portable electronic devices were provided early in this thesis. Based on the kinetics of acid promoted ammonia borane hydrolysis, feasible hydrogen reactor designs were presented and ranked against each other. Preliminary designs were experimentally tested and compared to simple pressure predicting models for performance and sensitivity to limiting factors.

An IV pressure infusion bag proved to be a robust method of delivering AB solution into a sealed reactor. Its simplicity makes such a design appealing for a fielded device. It was concluded that controlled exposure of solid AB must be pressure dependent in order to accommodate for the diverse loads put on a fuel cell. The issue with such a design is that all of the fuel, AB, is stored in the main reactor for the duration of the reaction. The consequence of a failed reaction would be high, with all the AB reacting at once. The liquid mixing design has the advantage of ensured stability over all solid AB designs.

It was identified that portable charging devices desired by the military will likely be used during rest periods on extended missions. The Army foot marching manual estimated that each soldier adds one 2590 battery every 10 hours for an infantry mission [11]. Figure 6.1 shows the expected weights that a soldier would carry using only 2590 batteries compared to the savings that a reactor/fuel cell charging system can provide. The charger's initial weight accounted for the system dry weight, a 2590 charge equivalent of reactants, a fuel cell of 0.814 lbs., and an individual power manager weighing 0.3 lbs. Since our system was designed to accommodate batteries rather than replace them, the expected weight is plotted for a soldier carrying two 2590's as well as the charger.

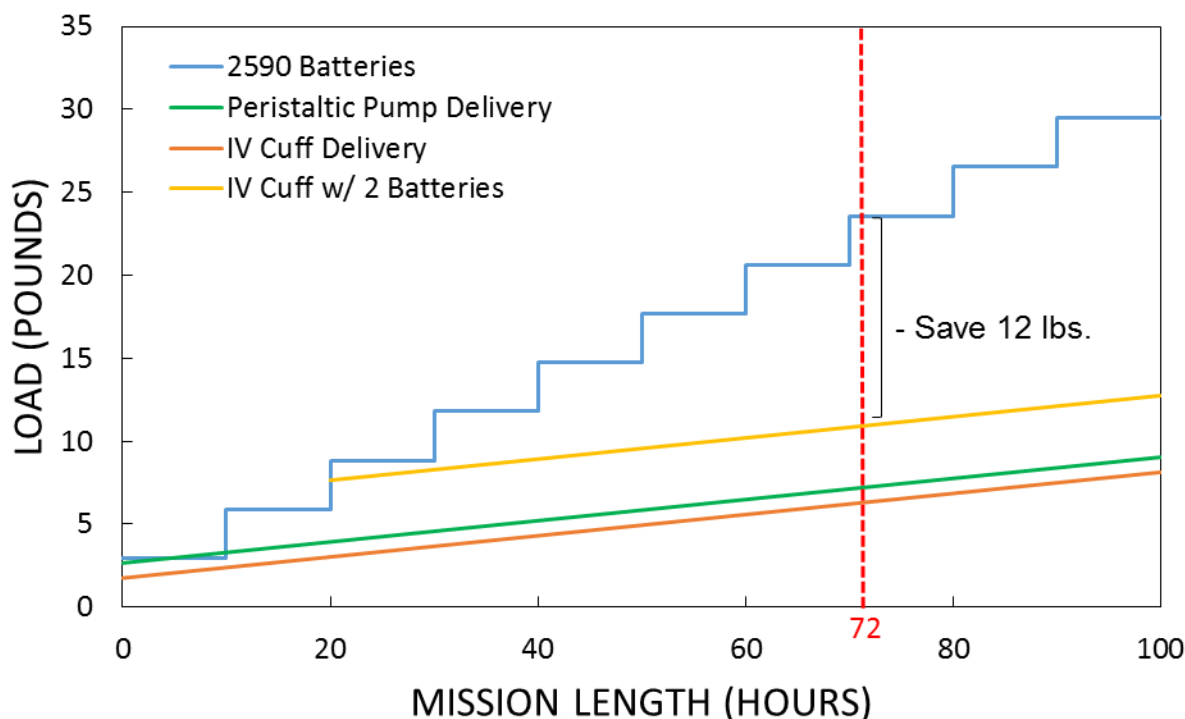


Figure 6.1. Mission length vs predicted load for individual soldier.

Compared to the peristaltic pump delivery scheme, the IV design's weight savings are negligible for longer duration missions. Given that the pressure cuff reactor is able to match the performance of the pump, its main advantage is in the simplicity of its components. The added dependence on the electrical and mechanical operation of a peristaltic pump makes such a reactor unappealing for small scale applications. Eliminating the peristaltic pump removes a point of potential failure. I would recommend the IV bag concept for a man portable reactor design. For a mission that has a 72 hour gap between resupplies, a soldier can save up to 12 lbs. when carrying our proposed system in addition to two 2590 batteries. The total volume of energy storage during such a mission would be reduced by 40 percent. Savings in weight and volume could extend the operational threshold for a soldier by allowing them to carry other essential equipment. From a squad perspective, these savings will be compounded, since only one person would be required to carry a reactor, fuel cell and power manager. Any individual not tasked with carrying a reactor will only have to carry the reactants required to charge their electronic devices. At 72 hours, individuals only carrying reactants will save another 1.5 lbs. Water was not factored into the weight assessment as it was assumed that it would be an in-situ resource. For this particular

system, approximately 3.4 lbs. or 1.5 liters of water would be required for each 2590 charge. The 1.5 liters was determined from the minimum allowable amount given in the temperature analysis in section 5.1.1 This amount of water could be reduced with heat control methods. The high dependence of this system on water reduces its practicality in environments with limited water supply.

Aside from portable devices, these reactor architectures could be useful to a variety of other applications. Within the military, robotics, drones and sensors containing “on board” spare batteries for extended operation could be hybridized to also hold a fuel cell reactor system. System scaling can also allow reactor designs to operate on a squad or company level rather than for just an individual. Even for units where weight is not an issue, a fuel cell can provide advantages over a generator such as noise reduction. The hydrolysis designs from Figure 3.1 not tested in this research could be used in non-man worn applications. The constant rate hydrolysis designs that required a buffering volume are viable for sensing systems that a warfighter will setup and leave in the field. For example, a large reactor with excess volume could be used to house the hydrolysis of a pellet in order to power thermal sensors in the field. Outside of the military, a robust chemical hydride reactor could have its place among disaster relief forces or commercial outdoor hobbyists.

6.1 Future Work

None of the reactor designs are past a technology readiness level of 4. There is still work to be done to experientially confirm the sensitivity analysis performed from the models. The MATLAB models can also be improved by considering reaction rate and its relationship to temperature and pH as the hydrolysis reaction progresses. Modeling the reaction kinetics of both liquid mixing and solid AB exposed to acid can be helpful. A limitation for all designs is the separation of hydrogen from solution at the delivery tubing to the fuel cell. A separation technique must be developed in order to make any of the reactors resilient towards orientation. Removing these reactors from the test stand will require a reliable method to ensure that air is not pressurized with hydrogen. Issues with air could be mitigated by the bag reactor’s small initial air volume but a purge procedure may be required. The purge can be performed by a rapid injection of AB to vent out air.

One of the prevailing challenges in optimizing all hydrolysis reactor designs is limiting the reaction temperature without sacrificing system weight. The current cooling method is adding

excess water to act as a heat sink. Future investigation can be done to optimize a cooling strategy and hopefully improve the reactor's energy density for a given charge duration. One system alteration that could help in cooling is directing the fan from the fuel cell to blow air over the reactor walls.

Another issue is the suspected inconsistency of AB stability. If AB is susceptible to ammonia off gassing, then all reactor designs with a dissolved AB could be ruled out. Experimentation with a fuel cell or FTIR has and will continue to be done to confirm these instabilities. Continued work on this project may either transition to another chemical hydride that is stable in solution or prioritize a solid AB pressure dependent design.

Once these points have been addressed, work can be done to develop the IV bag concept tested in this research into a durable system with military approved components. Once assembled, the reactor will be able to undergo validation described in section 2.4.1. On a system level, integration with a PEM fuel cell can be done at any point to identify any new performance characteristics. Pairing a finalized reactor model with a military grade PEM fuel cell is the last step in preparing a field able charging device for testing.

APPENDIX. MATLAB MODELS

Single Pressurization Code

```
clc
clear

gAB = 20;%[g] mass of AB per charge
VAB= gAB*5; % [ml] volume of water added to AB
purity = 1; %AB purity

con=gAB/VAB; %concentration of AB in water, [soluble at .26]
%VAB = gAB/.9*5.8; %ml, includes water VAB = gAB/.9/.26
nAB = gAB/30.865; %[moles] of AB
nAcid = nAB*1; %[moles] of Acid at 1 to 1 equivalence
MMacid = 116.07; %[g/mol], Maleic acid molecular weight
gAcid = nAcid*MMacid; %[g] mass of acid
Vacid = gAcid*11; %[ml] volume of acid added

V1= 5*VAB; %500; %ml, volume of AB delivery chamber
headspaceAB=V1-VAB; %initial headspace

V2=50+Vacid+VAB;%1000; %ml, volume of Reactor chamber
headspace=V2-Vacid; %Vacid; %V2*.7;% initial headspace

slpm=.7; %[SLPM] flow rate
flow=slpm*1000/60; %[ml/s]
rhoAB=(.7*con+(1-con)); %g/ml
nh2 = purity*nAB*3/VAB; %Moles of H2 per volume of AB, g/ml * molAB/g * molH2/molAB = molH2/mlAB
RT=8.314*298*1e6; %Pa*ml/mol 689.476; %ideal R, temp, volume constant (multiply by n and /V
for P)
ml_drop=.055; % ml per drop
totaldrops =VAB/ml_drop;% total drops expected given volume of AB solution

h=5*.0254; %[m], length of tubing to reactor
Dh=.0254/8; %[m], diameter of tubing, 1/8 inch
A=pi*Dh^2/4; %[m^2]
Do=.02*.0254; %[m], diameter of orifice
Ao=pi*Do^2/4; %[m^2]
Pcv=2*6894.76; %[Pa], cracking pressure of check valve was 4
visc=.000931; %[Pa-s], of water at 23 C

%initial conditions
Pab(1:3)=22.4*6894.76; %[Pa]22.4
Pc(1:3)=14.7*6894.76; %[Pa]
dP(1:3)=Pcv; %.333;
Vab(1:3)=VAB;
V1head(1:3)=headspaceAB;
V2head(1:3)=headspace;
VH2(1:3)=0;%154
nH(1:3)=101300*headspace/RT; %headspace*Pc(1)/RT;
```

```

d(1:3)=0; %initial drops
t(1:3)=0; %time = 0
ml(1:2)=0;

i=3;
dt=.1; %[sec] time step
while d(i) < VAB;
DP=Pab(i)-Pc(i)-dP(i); %Pressure drop between both chambers
DP(DP<0)=0;
mdot(i)=.6*pi/4*(Do)^2*(rhoAB*1000)*1000*(2*(DP)/(rhoAB*1000)*(1-(Do/Dh)^4))^0.5; %[g/s],
massflow of fluid
ml(i)=mdot(i)*dt/rhoAB+ml(i-1); %ml

%Pressure drop through delivery tube
dx=ml(i)/A*1e-6; %[ml/m^2]
vdot=(ml(i)/dt); %[ml/s]
V=vdot*1e-6/A; %m/s
Re=(rhoAB*1000)*v*Dh/visc; %[kg/m^3*m/s*m/Pa-s]
if Re>0
F=16/Re; % F=64/Re;
else
F=0;
end
kt=2.12; %Orifice loss coefficient
q1=(mdot(i)/1000)^2/(rhoAB/1000*1e6)/A^2/2; %[Pa] from kg^2/s^2 *m^3/kg /m^4
q2=(mdot(i)/1000)^2/(rhoAB/1000*1e6)/Ao^2/2; %[Pa]
dP(i+1)=Pcv + (rhoAB*1000)*9.8*h + q1*4*F*dx/Dh + q2*kt;
if ml(i) >=ml_drop
f=ml(i);
ml(i)=0;
else
f=0;
end

vdel(i)=f; %[ml] volume of solution AB %vdel(1)=d(1);
vab(i+1)= vab(i)-vdel(i);% volume of ab remaining
v1head(i+1)=v1head(i)+ vdel(i); %volume of IV headspace
v2head(i+1)= v2head(i)-vdel(i); %volume of chamber headspace

Pab(i+1)= Pab(i)*v1head(i)/v1head(i+1); %pressure drop in ab ?????? 2*
nadd(i+1)= vdel(i)*.1*nh2;%*((totaldrops-d(i))/totaldrops); %volume of hydrogen immadiatly made
ndelay(i+1)=vdel(i)*.2*nh2;
ndelay2(i+1)=vdel(i)*.3*nh2;
ndelay3(i+1)=vdel(i)*.4*nh2;
VH2(i+1)=nadd(i+1)/.1*RT/101300; %[ml]
if Pc(i) > 101300
on=1;
else
on=0;
end
nh(i+1)=nh(i)+ nadd(i+1)+ndelay(i)+ndelay2(i-1)+ndelay3(i-2)- on*(flow*dt)*101300/RT;
Pc(i+1)=nh(i)*RT/v2head(i+1); %vol(i) not sure what v to use
d(i+1)=d(i)+ f;
t(i+1)=t(i)+dt; %half second time step

```

```

i=i+1;
if Pc(i)< 101300
    Pab(i)=Pab(1);
    display('Re-pump')
end
end

nH(i)=Pc(i-1)*V2head(i-1)/RT +Pab(i-1)*V1head(i-1)/RT;
Vnew=V2head(i-1)+V1head(i-1);
Pcc=Pc(i);
while Pcc > 101300
    nH(i+1)= nH(i)-(flow*dt)*101300/RT;
    Pc(i+1)=nH(i)*RT/Vnew;
    Pcc=Pc(i);
    Pab(i+1)=Pc(i+1);
    t(i+1)=t(i)+dt;
    i=i+1;
end

LH2=sum(VH2)/1000
time=max(t)/60
maxP =max(Pc)
minP=min(Pc)
fontsize=14;

figure(2)
plot (t/60,Pc/6894.76,'r','Linewidth',1)
hold on
plot (t/60,Pab/6894.76, 'bl','Linewidth',2)
hold on
plot (t/60,14.7*ones(size(t)), 'r:','Linewidth',2)
xlabel('time [min]')
ylabel('Pressure [psia]')
hold on
set(gca, 'FontSize', fontsize)
legend('Reaction Chamber Pressure', 'AB Delivery Pressure', 'Atmospheric Pressure', 'location',
'northeast')

```

Regulated Hydrogen Fill Code

```

clc
clear

gAB = 10;%[g] mass of AB per charge
VAB= gAB*6; % [ml] volume of water added to AB
purity = 1; %AB purity

con=gAB/VAB; %concentration of AB in water, [soluble at .26]
%VAB = gAB/.9*5.8; %ml, includes water VAB = gAB/.9/.26
nAB = gAB/30.865; %[moles] of AB
nAcid = nAB*1; %[moles] of Acid at 1 to 1 equivalence

```

```

MMacid = 116.07; %[g/mol], Maleic acid molecular weight
gAcid = nAcid*MMacid; %[g] mass of acid
Vacid = gAcid*10; % gAcid*28; %[ml] Volume of acid added

V2=50+Vacid+VAB; %1000; %[ml], volume of Reactor chamber
headspace=V2-Vacid; %V2*.8;%Vacid;% initial headspace
Vd=headspace-140;%(gAB)/100*headspace
Vd(Vd<2)=2;
headspaceAB= 17.5*Vd/4.9;
V1=headspaceAB+VAB; % 600; %[ml], volume of AB delivery chamber
%headspaceAB=V1-VAB; %initial headspace

slpm=.72; %[SLPM] flow rate
flow=slpm*1000/60; %[ml/s]
rhoAB=(.7*con+(1-con)); %[g/ml]
nh2 = purity*nAB*3/VAB; %Moles of H2 per volume of AB, g/ml * molAB/g * molH2/molAB = molH2/mlAB
RT=8.314*298*1e6; %Pa*m1/mol 689.476; %ideal R, temp, volume constant (multiply by n and /V
for P)
ml_drop=.055; % ml per drop .04 matched better
totaldrops =VAB/ml_drop;% total drops expected given volume of AB solution
Preg= 22.4*6894.76; %psia
rhoH2= .0818; %kg/m^3

h=5*.0254; %[m], length of tubing to reactor
Dh=.0254/8; %[m], diameter of tubing, 1/8 inch
A=pi*Dh^2/4; %[m^2]
Do=.02*.0254; %[m], diameter of orifice
Ao=pi*Do^2/4; %[m^2]
Dreg=.035*.0254; %[m]
Areg=pi*Dreg^2/4;
Pcv=2*6894.76; %[Pa], cracking pressure of check valve
visc=.000931; %[Pa-s], of water at 23 C

%initial conditions
Pab(1:3)=22.4*6894.76; %[Pa]
Pc(1:3)=14.7*6894.76; %[Pa]
dP(1:3)=Pcv; %.333;
regdP(1:3)= .1*6894.76;
Vab(1:3)=VAB;
V1head(1:3)=headspaceAB;
V2head(1:3)=headspace;
VH2(1:3)=0;%154
nH(1:3)=101300*headspace/RT; %headspace*Pc(1)/RT;
d(1:3)=0; %initial drops
t(1:3)=0; %time = 0
ml(1:2)=.055;

i=3;
dt=.1; %[sec] time step
while d(i) < VAB;
DP=Pab(i)-Pc(i)-dP(i); %Pressure drop between both chambers
DP(DP<0)=0;
mdot(i)=.6*pi/4*(Do)^2*(rhoAB*1000)*1000*(2*(DP)/(rhoAB*1000)*(1-(Do/Dh)^4))^0.5; %[g/s],
massflow of fluid

```

```

m1(i)=mdot(i)*dt/rhoAB+m1(i-1); %m1

%Pressure drop through delivery tube
dx=m1(i)/A*1e-6; %[m1/m^2]
vdot=(m1(i)/dt); %m1/s
V=vdot*1e-6/A; %m/s
Re=(rhoAB*1000)*v*Dh/visc; %[kg/m^3*m/s*m/Pa-s]
if Re>0
    F=16/Re; % F=64/Re;
else
    F=0;
end
kt=2.12; %Orifice loss coefficient
q1=(mdot(i)/1000)^2/(rhoAB/1000*1e6)/A^2/2; %[Pa] from kg^2/s^2 *m^3/kg /m^4
q2=(mdot(i)/1000)^2/(rhoAB/1000*1e6)/Ao^2/2; %[Pa]
dP(i+1)=Pcv + (rhoAB*1000)*9.8*h + q1*4*F*dx/Dh + q2*kt;
if m1(i) >=m1_drop
    f=m1(i);
    m1(i)=0;
else
    f=0;
end

vdel(i)=f; %[m1] volume of solution AB %vdel(1)=d(1);
vab(i+1)= vab(i)-vdel(i);% volume of ab remaining
v1head(i+1)=v1head(i)+ vdel(i); %volume of IV headspace
v2head(i+1)= v2head(i)-vdel(i); %volume of chamber headspace
deltaP(i)= Pab(i)*v1head(i)/v1head(i+1); %pressure drop in ab ?????? 2*

ktreg=1.7; %Orifice loss coefficient
DPreg=Pc(i)-Pab(i);%regdP(i); %Pressure drop between both chambers
DPreg(DPreg<0)=0;
mdotH(i)=.6*pi/4*(Dreg)^2*(rhoH2)*(2*(DPreg)/(rhoH2)*(1-(Dreg/Dh)^4))^0.5;
qreg=(mdotH(i))^2/rhoH2/Areg^2/2; %[Pa]
regdP(i+1)=qreg*ktreg;
if Pc(i) > Preg + regdP(i+1)
    Pr=Preg;
else
    Pr=Pc(i);%(Pc(i+1))- dP(i);
end
Pab(i+1)= max(deltaP(i),Pr);

nadd(i+1)= vdel(i)*.1*nh2;%*((totaldrops-d(i))/totaldrops); %volume of hydrogen imeadiatly made
ndelay(i+1)=vdel(i)*.2*nh2;
ndelay2(i+1)=vdel(i)*.3*nh2;
ndelay3(i+1)=vdel(i)*.4*nh2;
VH2(i+1)=nadd(i+1)/.1*RT/101300; %[m1]
if Pc(i) > 101300
    on=1;
else
    on=0;
end
nH(i+1)=nH(i)+ nadd(i+1)+ndelay(i)+ndelay2(i-1)+ndelay3(i-2)- on*(flow*dt)*101300/RT -
on*(v1head(i+1)-v1head(i))*101300/RT;

```

```

Pc(i+1)=nH(i)*RT/V2head(i+1); %Vol(i)
d(i+1)=d(i)+ f;
t(i+1)=t(i)+dt; %half second time step
i=i+1;
if Pc(i)< 101300
    Pc(i)=Pc(1);
    %d(i)=totaldrops+2;
    display('Re-pump')
    d(i) = VAB;
end
end

nH(i)=Pc(i-1)*V2head(i-1)/RT +Pab(i-1)*V1head(i-1)/RT;
Vnew=V2head(i-1)+V1head(i-1);
Pcc=Pc(i);
while Pcc > 101300
    nH(i+1)= nH(i)-(flow*dt)*101300/RT;
    Pc(i+1)=nH(i)*RT/Vnew;
    Pcc=Pc(i);
    Pab(i+1)=Pc(i+1);
    t(i+1)=t(i)+dt;
    i=i+1;
end

LH2=sum(VH2)/1000
time=max(t)/60
maxP =max(Pc)
minP=min(Pc)
fontsize=14;

figure(1)
plot (t/60,Pc/6894.76,'r','Linewidth',1)
hold on
plot (t/60,Pab/6894.76, 'bl','Linewidth',2)
hold on
plot (t/60,14.7*ones(size(t)), 'r:','Linewidth',2)
xlabel('time [min]')
ylabel('Pressure [psia]')
hold on
set(gca, 'FontSize', fontsize)
legend('Reaction Chamber Pressure', 'AB Delivery Pressure', 'Atmospheric Pressure', 'location',
'northeast')

```

REFERENCES

- [1] J. Mattis, “Summary of the 2018 National Defense Strategy.” Department of Defense: The United States of America.
- [2] Office of the Assistant Secretary of Defense for Energy, Installations and Environment, “2016 DoD Operational Energy Strategy,” Department of Defense, 3400 Defense Pentagon Washington, DC 20301-3400, Dec. 2015.
- [3] “US Army Facts,” *Army*. [Online]. Available: https://www.army.mil/article/66277/us_army_facts.
- [4] “Fuel cells and other emerging manportable power technologies for the NATO warfighter.” NATO, Science and Technology Organization, 2014.
- [5] A. S. Patil *et al.*, “Portable fuel cell systems for America’s army: technology transition to the field,” *Journal of Power Sources*, vol. 136, no. 2, pp. 220–225, Oct. 2004.
- [6] A. Wahlman, C. T. Clavin, R. A. Keller, D. M. Georgi, and J. R. Ayers, “An Assessment of the Challenges Associated with Individual Battlefield Power: Addressing the Power Budget Burdens of the Warfighter and Squad,” Defense Technical Information Center, Fort Belvoir, VA, May 2014.
- [7] D. Cornel, “NEPTUNE Customer Discovery Interview,” 29-May-2019.
- [8] Bren-Tronics Inc., “Rechargeable Lithium-Ion Battery Technical Datasheet - BT-70791CK.” [Online]. Available: <https://www.bren-tronics.com/resource/datasheets/DS-BT-70791CK%20Rev%20C.pdf>.
- [9] “High Performance Rechargeable Lithium-Ion Battery Technical Datasheet - BT-70791CG.” [Online]. Available: <https://www.bren-tronics.com/resource/datasheets/DS-BT-70791CG%20Rev%20D.pdf>.
- [10] H. Jones, “SPECIAL OPERATIONS FORCES TACTICAL ENERGY RESOURCE (SOFTER),” Center for Army Analysis, 6001 GOETHALS ROAD FORT BELVOIR, VA 22060-5230, Dec. 2014.
- [11] Department of the Army, “Foot Marches-ATP 3-21.18 (FM 21-18).” Army Publishing Directorate, Apr-2017.
- [12] Marine Corps System Command, “SOLAR PORTABLE ALTERNATIVE COMMUNICATIONS ENERGY SYSTEM (SPACES).” [Online]. Available: <https://www.marcorsyscom.marines.mil/Portals/105/pdmeps/docs/APS/H0011.pdf>.
- [13] D. Braithwaite, C. A. Helland, T. G. DuBois, T. M. Thampan, and C. R. Schumacher, “Recent Achievements with Alane (Aluminum Hydride, AlH₃) and Fuel Cell Power Systems,” p. 4.
- [14] Army News and Media, “WEARABLE POWER SYSTEM,” *Center Corporate and Public Communication Office*. [Online]. Available: https://c5isr.ccdc.army.mil/news_and_media/Wearable_Power_System/.
- [15] SFC-Defense, “Product Flyer Jenny 600s.” [Online]. Available: https://www.sfc-defense.com/sites/default/files/product_flyer_jenny600s_online_en_2.pdf.
- [16] UltraCell, “XX25DMFC Data Sheet.” [Online]. Available: http://www.ultracell-llc.com/assets/XX25DMFC_Data_Sheet_SY011011-1_Rev_01.pdf.
- [17] S. R. Narayan and T. I. Valdez, “High-Energy Portable Fuel Cell Power Sources,” *The Electrochemical Society Interface*, p. 6, 2008.
- [18] SAFCell, “PP-50 Flex Portable Power System Datasheet.” [Online]. Available: <http://www.safcell.com/military>.
- [19] U.S. Department of Energy, “Fuel Cell Handbook (Seventh Edition),” p. 427.

- [20] P. P. Edwards, V. L. Kuznetsov, W. I. F. David, and N. P. Brandon, "Hydrogen and fuel cells: Towards a sustainable energy future," *Energy Policy*, vol. 36, no. 12, pp. 4356–4362, Dec. 2008.
- [21] P. Jena, "Materials for Hydrogen Storage: Past, Present, and Future," *The Journal of Physical Chemistry Letters*, vol. 2, no. 3, pp. 206–211, Feb. 2011.
- [22] U.S. Department of Energy, "Multi-Year Research, Development, and Demonstration Plan," Fuel Cell Technologies Office: U.S. Department of Energy, Aug. 2017.
- [23] S. McWhorter, K. O'Malley, J. Adams, G. Ordaz, K. Randolph, and N. T. Stetson, "Moderate Temperature Dense Phase Hydrogen Storage Materials within the US Department of Energy (DOE) H2 Storage Program: Trends toward Future Development," *Crystals*, vol. 2, no. 2, pp. 413–445, May 2012.
- [24] U. B. Demirci, "Ammonia borane in chemical hydrogen storage – Ammonia release during hydrolysis of ammonia borane, an issue," p. 10.
- [25] U. B. Demirci, "Ammonia borane, a material with exceptional properties for chemical hydrogen storage," *International Journal of Hydrogen Energy*, vol. 42, no. 15, pp. 9978–10013, Apr. 2017.
- [26] A. Brockman, Y. Zheng, and J. Gore, "A study of catalytic hydrolysis of concentrated ammonia borane solutions," *International Journal of Hydrogen Energy*, vol. 35, no. 14, pp. 7350–7356, Jul. 2010.
- [27] M. Chandra and Q. Xu, "Dissociation and hydrolysis of ammonia-borane with solid acids and carbon dioxide: An efficient hydrogen generation system," *Journal of Power Sources*, vol. 159, no. 2, pp. 855–860, Sep. 2006.
- [28] A. Karkamkar, C. Aardahl, and T. Autrey, "Recent Developments on Hydrogen Release from Ammonia Borane," *Material Matters*, vol. 2, p. 2, Sep. 2007.
- [29] N. Rajalakshmi, T. T. Jayanth, and K. S. Dhathathreyan, "Effect of Carbon Dioxide and Ammonia on Polymer Electrolyte Membrane Fuel Cell Stack Performance," *Fuel Cells*, vol. 3, no. 4, pp. 177–180, Dec. 2003.
- [30] X. Cheng *et al.*, "A review of PEM hydrogen fuel cell contamination: Impacts, mechanisms, and mitigation," *Journal of Power Sources*, vol. 165, no. 2, pp. 739–756, Mar. 2007.
- [31] T. B. Groom, J. R. Gabl, and T. L. Pourpoint, "Portable Power Generation for Remote Areas Using Hydrogen Generated via Maleic Acid-Promoted Hydrolysis of Ammonia Borane," *Molecules*, vol. 24, no. 22, p. 4045, Nov. 2019.
- [32] H. C. Kelly and V. B. Marriott, "Reexamination of the mechanism of acid-catalyzed amine-borane hydrolysis. The hydrolysis of ammonia-borane," *Inorganic Chemistry*, vol. 18, no. 10, pp. 2875–2878, Oct. 1979.
- [33] Revision Military, "Squad Power Manager (SPM-622)." [Online]. Available: <https://www.revisionmilitary.com/en/power/battery-systems/nerv-centr-squad-power-manager-spm-622>.
- [34] Protonex, "SPM-622 Squad Power Manager Datasheet." [Online]. Available: https://protonex.com/wp-content/uploads/2017/02/SPM-622_datasheet_2017_final.pdf.
- [35] Department of Defense, "MIL-STD-810: Test Method Standard: Environmental Engineering Considerations and Laboratory Tests." 31-Oct-2008.
- [36] Department of Defense, "MIL-PRF-32383: Performance Specifications Batteries." 16-Jun-2011.

- [37] N. S. Spinner, K. M. Hinnant, S. G. Tuttle, and S. L. Rose-Pehrsson, "Lithium-Ion Battery Failure: Effects of State of Charge and Packing Configuration:," Defense Technical Information Center, Fort Belvoir, VA, Aug. 2016.
- [38] P. Dai *et al.*, "Preparation, characterization, and properties of Pt/Al₂O₃/cordierite monolith catalyst for hydrogen generation from hydrolysis of sodium borohydride in a flow reactor," *International Journal of Hydrogen Energy*, vol. 44, no. 53, pp. 28463–28470, Nov. 2019.
- [39] A. Marchionni *et al.*, "High volume hydrogen production from the hydrolysis of sodium borohydride using a cobalt catalyst supported on a honeycomb matrix," *Journal of Power Sources*, vol. 299, pp. 391–397, Dec. 2015.
- [40] D.-W. Zhuang, H.-B. Dai, Y.-J. Zhong, L.-X. Sun, and P. Wang, "A new reactivation method towards deactivation of honeycomb ceramic monolith supported cobalt–molybdenum–boron catalyst in hydrolysis of sodium borohydride," *International Journal of Hydrogen Energy*, vol. 40, no. 30, pp. 9373–9381, Aug. 2015.
- [41] A. Gutowska *et al.*, "Nanoscaffold Mediates Hydrogen Release and the Reactivity of Ammonia Borane," *Angewandte Chemie International Edition*, vol. 44, no. 23, pp. 3578–3582, Jun. 2005.
- [42] Z. Yang, J. Liang, F. Cheng, Z. Tao, and J. Chen, "Porous MnO₂ hollow cubes as new nanoscaffold materials for the dehydrogenation promotion of ammonia-borane (AB)," *Microporous and Mesoporous Materials*, vol. 161, pp. 40–47, Oct. 2012.
- [43] S. Govender and H. Friedrich, "Monoliths: A Review of the Basics, Preparation Methods and Their Relevance to Oxidation," *Catalysts-MDPI*, Feb. 2017.
- [44] P. V. Ramachandran and A. S. Kulkarni, "Water-promoted, safe and scalable preparation of ammonia borane," *International Journal of Hydrogen Energy*, vol. 42, no. 2, pp. 1451–1455, Jan. 2017.